G.U. AERO REPORT 9201

CONTRACT REPORT

for

THE SCIENCE AND ENGINEERING RESEARCH COUNCIL

CONTRACT NUMBER GR/F/06760

by

R. A. McD. GALBRAITH

M. W. GRACEY

E. LEITCH

Department of Aerospace Engineering
University of Glasgow
Glasgow
G12 8QQ

Tel. 041 330 5295
Fax. 041 330 5560

JANUARY, 1992.

G.U. AERO REPORT 9201

CONTRACT REPORT

for

THE SCIENCE AND ENGINEERING RESEARCH COUNCIL

CONTRACT NUMBER GR/F/06760

by

R. A. McD. GALBRAITH

M. W. GRACEY

E. LEITCH

Department of Aerospace Engineering
University of Glasgow
Glasgow
G12 8QQ

Tel. 041 330 5295
Fax. 041 330 5560

JANUARY, 1992.

SUMMARY

This document constitutes the final report for SERC award No. **GR/F/06760**. It first details the work programme of the original proposal made in 1987 and notes the work done to illustrate completion and extensions beyond that proposed. For brevity, we confine the technical discussion to the salient features of a particular aerofoil, albeit the work was an integral part of a larger programme on dynamic stall. The extent of this work may be gleaned from the accompanying enclosures representing some recent activity at Glasgow University.

Two of the main technical results from the present authors are worthy of note in that the first (i.e. a correletion for incipient dynamic stall) has been used both in industry (VAWT Ltd) and research (under **SERC GR/F/63466**) to propose new aerofoil shapes for wind turbines. The second, however, (negative lift at large incidence during ramp-down motions from the stalled condition) has generated a new research activity (funded under **SERC GR/H16711**). This and future prospects are discussed prior to the concluding remarks. These remarks express the authors opinion of the success and overall value of the programme.

CONTENTS

NOMENCLATURE

A, B, C, D	coefficients in correlation equation
$C_m, C_{m1/4}$	coefficient of pitching-moment about quarter-chord location
C_n	coefficient of force normal to chord
C_n'	ersatz coefficient of force normal to chord
C_{n1}	critical coefficient of force normal to chord
C_p	coefficient of pressure
c	length of chord
c_1, c_2, c_3	constants in derivation of correlation equation
$F_1(.)$	general function relating m_1 and m_2
f	separation point in form of x/c
f_{max}, f_{min}	constants in separation point equation
i, j	parameters in correlation equation
K_1, K_2	constants in separation point equation
k	reduced frequency
m_1, m_2	constants in derivation of correlation equation
p	Laplace variable
R	Reynolds number x 10^{-6}
r	reduced pitch-rate, calculated from $(d\alpha/dt)c/2U_\infty$
S_1, S_2	constants in separation point equation
T_p	pressure compensation time constant
t	time in seconds
U_∞	freestream velocity
x	coordinate in direction of aerofoil chord
α	angle of attack
α_1	constant in separation point equation
α_a	amplitude in oscillatory cycle
α_c	critical angle of attack
α_{ds}	incidence of C_p deviation
α_{ss}	incidence of steady stall
γ	gamma function for Gormont model
Δt	time delay in seconds
$\Delta\alpha$	change in angle of attack
$\Delta\alpha_d$	incidence delay between steady and dynamic stall
$\Delta\tau$	non-dimensional time-delay expressed in chordlengths of travel as $\Delta t.U_\infty/c$
ζ	pitch-damping parameter
τ^*	non-dimensional time-delay between analogous critical angle of attack and incidence of C_p deviation

1 INTRODUCTION

Current interest in the phenomenon of dynamic stall is found primarily in the both the helicopter and vertical-axis wind-turbine industries. The phenomenon is also recognised as an important consideration in stall regulated horizontal axis wind-turbines whilst operating in yawed conditions. Additionally, high maneouvrability aircraft hope to utilise unsteady aerodynamic augmentation to enhance their overall performance. Finally, new generations of aircraft, with gust alleviation, may enter the domain of unsteady aerodynamics associated with the control surface movement and aircraft response. Primarily, of course, the present work is concerned with unsteady aerofoil motions akin to helicopter rotors and "H" configured vertical-axis wind-turbines.

Over the past decade several aerofoils have been tested under unsteady aerodynamic conditions at Glasgow University; the majority of these are summarised in **Reference 1**. Two main families of aerofoils have been considered the first of which was based on the NACA 23012 and included three derivatives. The main incentive for this particular family came from an interest in the dynamic stall of helicopter rotors. The second was a selection of six symmetric sections ranging from a NACA 0012 to a NACA 0030. These were tested as part of a performance assessment associated with vertical-axis wind-turbines.

The design, construction and testing of these aerofoils was a long and demanding task for a small team. Typically each aerofoil would have up to 500 test cases resulting in the necessary archiving of approximately 20 million data samples per model. All the aerofoils were tested over an extended period of time and, given the normally fixed duration of projects and the continual updating of equipment and software by various researchers, the data presentation and data analysis software were not in a well-documented or consistent form.

Unlike many other experiments, much data were recorded because of the then test difficulties, in the knowledge that they would only be analysed by future researchers. After testing ten models, the need for a controlled and standard documentation and archiving became acute. It was also decided that

other data, e.g. blade vortex interaction, should be treated similarly. Hence the work proposed for the programmer as detailed in **Figure 1**.

Additionally the contractual pressure to acquire data left little time for detailed formal analysis, other than discussions of salient features and obvious differences betwen the aerofoils. This was disappointing and, hence, the major activity of the research assistant was to start detailed analysis of the database and provide a consultancy service on that data.

All the tasks detailed in the original proposal have been completed and whilst many of them can be assessed objectively, the database for example, the detailed analysis cannot. This is because it requires a quality judgement.

Several researchers have been involved in the detailed analysis and whilst an overall approach to the work will be discussed, only that which was the main interest of the current research assistant (Dr M Gracey) will be detailed. The overall work has produced 16 papers and 21 contract reports during the 3 year period.

In summary, three main areas of investigation provided useful design data, anomalous results or interesting and as yet unexplained phenomena. These were

a)	a correlation for stall onset (design information)	**Figure 2**
b)	anomalous results for stall vortex convection	**Figure 3**
c)	negative lift at large positive incidence during ramp-down motions	**Figure 4**

The correlation (a) for stall onset has been used in subsequent work (**SERC GR/F/63466**), and VAWT Ltd) to design aerofoil sections specifically for stall regulated vertical-axis wind-turbines. Additionally, associated investigations highlighted inconsistencies in current modelling algorithms for such conditions and provided a link between data for both oscillatory and constant pitch-rate ramp motions.

After stall onset, the build up and convection of a stall vortex has been extensively investigated under USA-AFOSR Contract No 89-0397A and, albeit Glasgow had access and now posesses raw data from similar dynamic stall tests performed at URTC (Contract **AFOSR-89-0397 A**), there remains the following anomaly: the Glasgow data, and others, suggest that the convection velocity of the stall vortex is, to a first order, independent of aerofoil motion, whilst that of URTC, and others, suggest the opposite (**Figure 3**). Unfunded work is continuing on this topic.

During the present work it was noticed that, for high speed ramp-down motions from the stalled condition, there may exist negative lift at large positive incidence (eg 10^{o}). The authors believe that this is the first recognition of the phenomenon and, whilst one can speculate on why this should be so[2], the available data are insufficient to provide a confident description of the associated flow states. The work continues and includes lowspeed flow visualisation, highspeed flow visualisation and high aspect ratio model tests. Funding for the work has been provided by the SERC under grant number **GR/H16711.**

Perhaps the most used result so far, however, has been the correlation for stall onset and the associated comparison with modelling algorithms. As was mentioned above, this has been incorporated in the aeofoil design code and been used, both by the University and VAWT Ltd, to consider aerofoil shape modifications in the region of the leading edge to produce an early stall. The requirement for this is simply to place such sections in the crossarm region of an H-configured vertical-axis wind-turbine and so force preferential stalling in that region. This, hopefully, will reduce any out of balance bending moments at the crossarm due to out of phase stalling at the blade tips.

As may be gleaned from the above, the field of work is active, productive and attracts industrial support. It therefore continues, and details of future prospects are given.

2 DETAILS OF THE WORK COMPLETED AS PER THE ORIGINAL PROPOSAL

2.1 Introduction

In the original proposal of 1988, the detailed description and sequence of the work programme was presented; the succinct summary of this is given in **Figure 1**. The work was loosely split between a researcher and a programmer. The researcher having responsibility for dynamic stall modelling and data analysis whilst that of the programmer was to set up database management procedures and the documentation of associated software. It is the purpose of this section to go through each of the proposed activities and indicate the state of completeness.

2.2 Work Completed by Programmer

Transfer and Archiving of Dynamic Stall Data

The data produced from dynamic stall experiments have been loaded on to the University of Glasgow's aerofoil database. Data files which are relevent to current research are easily accessed via a DEC MICROVAX 3400. Data files from the complete series of experiments are stored on both microcassette, for use on the MICROVAX 3400, and magnetic tape media, for use on a DEC Local Area VAX cluster. This VAX cluster consists of one VAX 8250 and two MICROVAX 3600 machines which are linked together with appropriate tape drives and printer, communicating over an Ethernet network. The data are catalogued by both aerofoil and motion type, and are stored both as raw voltages and reduced pressure coefficient values. Data are loaded and archived as each new model is tested so that analysis may begin immediately. Data from thirteen aerofoils have been loaded and archived in this manner.

For the study of dynamic stall on helicopter rotor blades, a family of aerofoils derived from the NACA 23012 section have been tested. In addition to the original aerofoil, the family consists of the 12%-thick NACA 23012A and NACA 23012C sections, which are identical to the NACA 23012 over the leading 25% chord but modified downstream of this location to produce reflex trailing-edge camber and greater positive camber respectively, and the NACA 23012B, which is a 16% thick composite aerofoil derived from the NACA 23012 and an RAE section. For the study of vertical-axis wind-

turbines, six NACA 4-digit symmetrical aerofoils (NACA 0012; NACA 0015; NACA 0018; NACA 0021; NACA 0025; NACA 0030) were tested. To consider wind-tunnel effects, a NACA 0015 aerofoil with a chord length half that of the original was tested. In addition, Cranfield Institute of Technology and VAWT Ltd have each provided an aerofoil for testing.

Transfer and Archiving of Blade-Vortex Interaction Data

A series of blade-vortex interaction experiments has been performed on a NACA 0015 aerofoil with an updated data acquisition system, the establishment of which was part of the work proposed. The data are now converted by a THORN-EMI BE256 unit and logged via an IBM PSII80 microcomputer on a 2000 megabyte IBM "WORM" optical disc. The reduced pressure data have been loaded and archived in the same manner as for dynamic stall. In order to record, transfer, load and archive the data by this new procedure, all software has been updated.

Archiving of Low Reynolds Number Data

Models of the NACA 0015, NACA 4415, GA(W)-1 and GU25-5(11)8 aerofoil sections have been tested at Reynolds numbers between 50,000 and 500,000. Because of the nature and use of these data, they have not been archived as with the BVI or DS data. Currently the data are not used in a similar way to the unsteady aerodynamic data and so are retained in their original form as this is deemed the most economical procedure meantime.

Ugrading of Data Acquisition Systems

Work is "on going" on upgrading data acquisition procedures and software with the aim that data should be recorded and analysed in the same way for both dynamic stall and blade-vortex interaction experiments. All software for data acquisition, transfer and access from storage spaces are currently being documented in order to satisfy the requirements, which have been established by past and current users.

2.3 Work Completed by Research Assistant

All the proposed work contained in **Figure 1** has been completed. In particular, a variety of dynamic-stall models have been coded and, as will be seen in **Section 3.7**, have been compared with

data from the Glasgow database. After careful consideration, the Beddoes model was incorporated in the Glasgow aerofoil design package and likewise the derived form of a stall onset correlation.

In the light of the analysis of Glasgow University's data, the timing of stall onset in the Beddoes model has been adjusted to yield better correspondence between the reconstructed and measured data. This modified model has been incorporated in two vertical-axis wind-turbine performance codes. First, a fixed wake model and, second, a prescribed wake model developed under a separate SERC award (**SERC GR/F/63466**). Consultations have taken place with both Westland Helicopters and VAWT Ltd pertaining to the results contained in **Section 3**. Although not explicitly mentioned in **Figure 1**, analysis of special features of the data was implicit in the proposal and details of that are contained in **Section 3** below.

Aerofoil Design

The NACA 23012C aerofoil section (**Figure 5**) was designed with the aid of a large number of FORTRAN algorithms which have subsequently been incorporated into the University of Glasgow's aerofoil design package[3]. An earlier report for S.E.R.C. contract **GR/D/41064** described its design, the construction and instrumentation, improvements to the data acquisition system, the calibration and testing, presentation of the data and a brief review of the early analysis of the data. These data have enabled research to be performed by a number of researchers on characteristics in steady and unsteady conditions, with particular emphasis on dynamic stall onset and reattachment. The data produced by the NACA 23012C were compared with similar data from experiments on other aerofoils, in particular the NACA 23012.

Aerofoil Test Procedures

The test procedures have been described in detail in companion reports (e.g. **Gracey and Galbraith[4,5], Angell et al[6]**). The tests were performed in the University of Glasgow's low-speed "Handley-Page" wind tunnel. This is an atmospheric closed-return tunnel with a 5'3" x 7' (i.e. 1.61m x 2.13m) octagonal working section in which a wind velocity of 61ms^{-1} can be attained. The aerofoils were tested in both steady and unsteady conditions over a Reynolds number range of between

$1.0x10^6$ and $2.0x10^6$. In unsteady conditions, the aerofoil was subjected to number of motion types, these included sinusoidal, a vertical-axis wind-turbine simulation and constant pitch-rate motions in both positive ("ramp up") and negative ("ramp down") directions. Data were recorded as pressure readings at thirty locations around the aerofoil's surface. The aerodynamic coefficients were subsequently calculated by suitably integrating the pressure data. Unless otherwise stated, all the data were averaged over a number of cycles, normally ten for oscillatory and five for constant pitch rate motions.

2.4 Concluding Remarks

All the proposed work of the researcher and programmer have been completed and, as will be discussed below, extended. The University of Glasgow now has a useful and extensive database which is easily accessible by any member of the research team or authorised user. Data have already been transferred to Vertical Axis Wind Turbines Ltd, Westland Helicopters and the Cranfield Institute of Technology. Additionally, as the database becomes more widely known, we anticipate increased interest from the United States of America where we already have close collaboration with the United States Air Force Academy, University of Boulder Colorado, University of Maryland, NASA AMES and AFOSR.

3 SALIENT RESULTS OF PRESENT ANALYSIS

3.1 Introduction

The work described in the present section is a grouping of analyses which have primarily been performed under the present contract. All work contributed to by other researchers is acknowledged. Accordingly, the basic analysis of the aerofoil designed by the researcher is considered before discussing associated aerofoils. The Section includes a discussion on the duration of dynamic stall, the onset of dynamic stall, comparison of various modelling algorithms and the method by which the Wilby criterion for criticality can be extended to ramp-up motions.

Coding of Predictive Algorithms

A version of Beddoes's second-generation model has been coded[7] and combined with the University of Glasgow's prescribed-wake model[8,9] to form a single algorithm for predicting vertical-axis wind-turbine performance. This version of the model has been based on the paper of **Leishman and Beddoes**[10], with additional references to papers of **Leishman**[11,12,13]. Since all current work was at low Mach numbers, the definition of stall onset (**Beddoes**[14]) based on **Evans and Mort's**[15] correlation, was always invoked. Additionally it was found necessary to make a few minor model modifications to reconstruct the Glasgow data. For example, the modelling of separation loci by a more general form[16] of the exponential equations has been beneficial.

This slightly modified algorithm can be used in combination with the University of Glasgow's aerofoil design package[3] to explore new aerofoil shapes for vertical-axis wind-turbines. In conjunction with field data provided by VAWT Ltd, two new aerofoils with an early stall have been proposed and are currently under test.

Whilst the Beddoes model was preferred, several other algorithms were coded; these are discussed in **Section 3.7**. Additionally a discrete vortex method is being developed specifically as a tool to assist the data analysis and assess tunnel constraints.

Software for Data Analysis

To assist the efficient analysis of the data, a suite of FORTRAN routines has been coded and documented. This task involved consulting other researchers regarding their personal software suite and re-configuring appropriate files into the general package. All the software and the files containing documentation are stored in a central space which can be accessed by all members of the research group. Only formally documented software is permitted in the package.

3.2 Basic Analysis of NACA 23012C Aerofoil Data

In steady conditions, typical and expected aerodynamic performance was observed (**Figure 6**). As intended, the separation characteristics of the NACA 23012C aerofoil were more typical of an aerofoil experiencing trailing-edge stall than those of the NACA 23012. As a result of these separation characteristics, and as would be anticipated of an aerofoil whose maximum camber was located further aft, the NACA 23012C stalled less abruptly than the NACA 23012. Additionally the NACA 23012C possessed a zero-lift incidence of -2.8° as compared to -0.7° and 1.0° for the NACA 23012 and NACA 23012A respectively. The NACA 23012C and NACA 23012 aerofoils possessed similar normal-force coefficient curve slopes. Also, and primarily associated with the enhanced leading-edge camber, the NACA 23012C exhibited a higher maximum normal force, higher stall incidence and larger magnitude of negative pitching-moment both before and after stall. The pre-stall magnitudes of quarter chord pitching-moment were approximately -0.08 and -0.01 for the NACA 23012C NACA 23012 respectively.

The most important parameters in the dynamic stall process were reduced pitch-rate and, in the oscillatory experiments, maximum incidence. As reduced pitch-rate increased, the magnitudes of the loads increased and the incidence at which events occurred was increasingly delayed. In addition, when stalling at low reduced frequencies and pitch-rates (i.e. $\mathbf{k}<0.03$, $\mathbf{r}<0.01$), there was little evidence of the dynamic stall vortex. At higher frequencies, as observed in deviations in the gradients of the pressure and normal force histories (as described in **Section 3.4**), the dynamic stall vortex greatly influences the aerodynamic characteristics and plays a significant role in the dynamic stall process.

Over the range of tests to which each aerofoil was subjected, the NACA 23012C consistently possessed the greatest magnitudes of maximum force and highest incidence for the occurrence of each event. However, after stall was initiated, the NACA 23012C experienced by far the most severe fluctuations in its airloads.

The NACA 23012C was observed to possess a number of favourable properties. Unfortunately, because of its large pitching-moment magnitudes and its severe post-stall characteristics, it is unlikely to be employed in practice. However the data produced by the NACA 23012C has proved very important in the analysis discussed below.

3.3 Aerodynamic Damping

Aerodynamic damping is a consequence of the hysteresis loops which result, in oscillatory experiments, and as described by **McCroskey**[15], a measure of this aerodynamic damping for one complete cycle is provided by the pitch-damping parameter ζ, defined as

$$\zeta := -\int_c C_m \, d\alpha / 4\alpha_a^2, \qquad (1)$$

where α is the angle of attack, α_a the amplitude of oscillation, and **c** the pitching moment verses incidence cycle. The integral term in **(1)** represents the net area enclosed by the cycle. It can be shown that the contribution to the pitch-damping parameter is positive from an anticlockwise loop and negative from a clockwise loop. If the pitch-damping parameter is negative (known as "negative damping"), the aerofoil extracts energy from the airstream, leading, if unrestrained, to stall flutter.

Figure 7 illustrates the variation of the pitch-damping parameter with maximum incidence for the NACA 23012C at each reduced frequency for a Reynolds number of 1.5×10^6. In fully attached conditions, the value of the pitch-damping parameter increased with reduced frequency, reflecting the increasing degree of hysteresis. However, once the aerofoil moved into stalled conditions, this variation was complicated by the growing influence of the dynamic stall vortex.

At the lower reduced frequencies the C_m loops were similar to the steady flow case and illustrated in **Figure 8(a)**. This produced a sizeable clockwise loop giving negative damping at the higher frequencies where it became more pronounced.

For reduced frequencies of 0.10 and greater, this trend changed because of a strengthening dynamic-stall vortex. The influence this had on the pitching-moment trace may be seen in **Figure 8(b)** as a range of large negative values in the higher incidence loop. Generally the magnitude of the minimum pitching moment increased with increasing reduced frequency over the test range considered. In addition, as will be discussed later, the rate at which the vortex was convected across the aerofoil was relatively independent of aerofoil motion. Consequently, and for particular cases, a lower incidence could be reached on the downstroke before the vortex was shed from the trailing-edge. Both of the above phenomena increased the area of the clockwise hysteresis loop and, hence, reduced the value of the pitch-damping parameter. At reduced frequencies of 0.150 and and 0.175, the effect was sufficient to achieve negative pitch-damping.

As illustrated in **Figures 9** and **10**, these characteristics were also typical of the NACA 23012 and NACA 23012A aerofoils. Like the NACA 23012C, the NACA 23012A possessed a large range of reduced frequencies for which the pitch-damping parameter remained positive ($0.025 \leq k \leq 0.127$ for the NACA 23012C; $0.026 \leq k \leq 0.105$ for the NACA 23012A). However, the NACA 23012 exhibited regions of negative damping at all reduced frequencies.

The above observations are in keeping with those of **McCroskey**[17] and **Dadone**[18], who found that positive damping is favoured in conditions in which stall is gradual.

3.4 Dynamic-Stall Vortex-Inception

Several methods[19] have been employed to determine the timing of incipient dynamic stall. Some of these methods have involved the examination of airloads. However, as a consequence of the airloads being calculated in the present procedure by integrating the recorded pressure coefficient values around the surface of the aerofoil, early indications of incipient stall may be disguised or hidden : during vortex initiation it is likely that the formation of any localised disturbance within the boundary layer would be indicated immediately by the response of the local pressure coefficient, whereas the

integrated airloads would de-sensitise the inception point. It was, therefore, decided that the onset of stall should be examined in relation to individual pressure traces.

A number of methods involving pressure traces have been employed by other researchers[19]. Among them were **Seto and Galbraith**[20] when testing the NACA 23012 aerofoil under ramp motion in the manner established for testing at the University of Glasgow. They established a criterion for indicating that the stall process had been initiated and could not be reversed. This criterion was employed as follows in the present analysis.

Seto and Galbraith described the ramp data lying in two mutually-exclusive regimes. At low reduced pitch-rates, where the characteristics are qualitatively similar to those in steady conditions with significant lift and moment overshoot, the response is labelled "quasi-static". The limit to the quasi-static behaviour of stall was observed to be at a reduced pitch-rate of approximately 0.01. At higher reduced pitch-rates, the dynamic stall vortex plays a significant part in the stall process and the response is associated with "dynamic" stall.

The first indication that this dynamic stall vortex had been initiated was when a deviation in the gradient of one of the pressure coefficient traces was observed. The incidence at which this deviation occurred was defined (**Figure 11**) as being the intersection of two straight lines which had been determined from linear regression through data points immediately before and after stall onset. Dynamic stall is distinguished from quasi-static stall by the presence of this deviation in the pressure coefficient trace. Hereafter, this response will be referred to as C_p deviation. The first transducer to reveal C_p deviation was found to vary with aerofoil. Its range in the aerofoils examined has been between 25% and 60% chord, and occurred at 27% chord on the NACA 23012C. The incidence of C_p deviation was observed to vary approximately linearly with reduced pitch-rate, as illustrated for the NACA 23012C at a Reynolds number of 1.5×10^6 in **Figure 12**. The gradient of this line increased with Reynolds number and varied with aerofoil geometry.

Using the current procedures and definitions of incipient dynamic stall, this C_p deviation (and its associated incidence) is the earliest indication which can be detected from the examination of the pressure histories, that a consequence of stall, which cannot be reversed, has occurred. Evidence discussed by **Niven**[21] shows that it is not the stall trigger, but it is the earliest indication which can be

observed from experimental data based on pressure readings from aerofoils experiencing trailing-edge stall at low Mach numbers.

There appeared to be a correlation between the incidence of C_p deviation and the maximum pitch-rate attained during tests of any type of motion. Of interest is the fact that the maximum reduced pitch-rate for a test at a reduced frequency of 0.03 is approximately 0.01. These values are approximately those at which the dynamic stall vortex began to play a prominant role in the dynamic stall process.

3.5 The Duration of Dynamic Stall Events

The dynamic stall process was observed to consist of a number of events, clearly displayed during ramp tests on the NACA 23012C aerofoil. There was a distinct and steady increase with non-dimensional time in normal force, the magnitude of pitching moment and leading-edge suction over the initial period of the ramp. After incipient separation of the boundary layer, there followed the initiation of the dynamic stall vortex. The first indication of the influence of this vortex was revealed as a deviation of the pressure coefficient trace at the 27% chord location. As the motion continued, and the vortex grew in strength, there was a deviation in the gradient of the normal coefficient trace. The suction at the leading edge then collapsed and the dynamic stall vortex was shed downstream. As the vortex moved towards the trailing-edge, each pressure transducer in succession registered a peak in the suction at its location, and the magnitude of pitching moment at first increased and then was reduced. The maximum magnitudes of the coefficients of normal force and pitching moment were attained while the vortex was being shed downstream.

This sequence of events summarises the dynamic stall process. However, in order to model the process, the time taken between each incident must be determined. Five important angles of attack which are easily measurable are: static-stall, C_p deviation (mentioned above), the maximum value of peak suction at the leading-edge, initiation of vortex shedding from the location of its inception and the release of the dynamic stall vortex from the trailing edge. **Table 1** lists the variation with reduced pitch-rate of the non-dimensional time, measured in chordlengths of travel, which passed between the

occurrence of these events. In addition, the delays between neighbouring events are illustrated in **Figure 13**. It can be seen that the non-dimensional time-delays were not, in general, independent of aerofoil motion. The delays between C_p deviation and both the shedding downstream of the dynamic stall vortex from that chord location and the maximum peak suction being attained at the leading edge were not constant. It appears that the strength of the vortex increased with reduced pitch-rate but that the rate at which it grew was relatively independent of aerofoil motion. This latter claim is supported by the fact that the trace of C_p deviation against reduced pitch-rate was observed to be approximately linear for all aerofoils tested at the University of Glasgow, and, hence, the gradient did not vary significantly with reduced pitch-rate. All subsequent non-dimensional time-delays were relatively independent of reduced pitch-rate. These constant delays included the non-dimensional time taken to move downstream to any location, as indicated by suction peaks at each transducer. The independence of the rate of vortex shedding with repect to aerofoil motion has been supported by subsequent research on all the aerofoils on the database by **Green et al**[22]. It can therefore be seen that, once C_p deviation was observed, the dynamic stall vortex grew in strength in proportion to the reduced pitch-rate for a non-dimensional time which was a linear function of reduced pitch-rate and was then shed downstream at a velocity which was independent of aerofoil motion.

It was also observed that the time which elapsed between passing through the steady stall incidence and each of the other events occurring was not independent of pitch rate. In particular, the delay between reaching the steady stall incidence and the C_p deviation being observed was a linear function of reduced pitch-rate. However, by examining the stall criterion of **Beddoes**[10,14], this delay can be broken down into two shorter delays.

Beddoes postulated that, under low-speed fully unsteady conditions, dynamic stall is triggered at the leading edge. As a result, to calculate an idealised steady stall incidence, he employed **Evans and Mort's**[15] correlation in which aerofoils are assumed to experience leading-edge stall by the reseparation mechanism. This incidence is that at which the leading-edge becomes critical, and is calculated theoretically by suppressing all trailing-edge separation. The dynamic stall onset incidence is determined as the angle of attack which the aerofoil reaches after the expiry of the relevant non-dimensional time-delay since pitching through this equivalent steady stall incidence. In practice, a critical normal force coefficient value C_{n1}, associated with the incidence at which the leading-edge

pressure criterion is invoked, denotes dynamic stall onset. From unsteady aerofoil tests, Beddoes has observed that, under nominally attached flow conditions, there is a lag in the leading-edge pressures with respect to the normal force. He illustrated that the simplest representation of this behaviour was via a first order lag with a Mach-number-dependent time-constant T_p. As a result, it is possible to relate the pressure in the unsteady flow to that in steady conditions by applying a lag to the value of normal force, producing a value C_n'. In the Laplace domain, this relationship can be expressed as

$$C_n'(p)/C_n(p) = 1/(1+T_p p),$$

where **p** is the Laplace variable. In the time domain, the dynamic stall process is regarded as being initiated at the angle of attack where $C_n'(t)$ is equal to the critical normal force coefficient C_{n1}. The non-dimensional time-delay between dynamic stall onset as defined by this criterion (from results produced by the program described in **Section 3.1**) and the earliest observed indication of vortex initiation, C_p deviation, is plotted against reduced pitch-rate in **Figure 14**. It can be seen that the delay is approximately independent of aerofoil motion.

Therefore the dynamic stall process has been observed as consisting of a number of sub-processes. The delay between the incidences of steady stall and dynamic stall incidence as defined by Beddoes is dependent on Mach number, and the delay between incurring stall in this form and the vortex being observed from pressure data is independent of reduced pitch-rate. As described above, the dynamic stall vortex then grows in strength for a length of time which is proportional to reduced pitch-rate and is shed downstream at a velocity which is independent of aerofoil motion.

3.6 A Correlation for Incipient Stall under Ramp Motions

As described in **Section 3.4**, the incidence of C_p deviation varied with reduced pitch-rate, Reynolds number and aerofoil geometry. This section describes a method by which these relationships may be represented by a single equation. The task involves parameters, derived from the results of experiments or predictive codes in steady conditions, which are unique to each aerofoil.

With the aid of a numerical boundary-layer model, **Scruggs et al**[23] demonstrated that there was a high degree of correlation between the incidence at which significant flow reversal reached the 50% chord location and the experimentally-measured incidence of dynamic stall onset. This model also predicted that, as pitch-rate increases, so does the extent of the delay in flow reversal and the rate of the subsequent forward movement of the flow-reversal point.

Water tunnel experiments by **McAlister and Carr**[24] revealed that, prior to vortex formation, a region of reversed flow momentarily appeared over the entire upper surface without any appreciable disturbace to the viscous-inviscid boundary. **McCroskey et al**[25,26] observed that, for aerofoils exhibiting gradual trailing-edge stall, vortex initiation was preceded by a gradual forward movement of flow reversal in a thin layer at the bottom of the boundary layer. Since no upper surface pressure divergence, which would have indicated possible boundary-layer separation, was observed, this behaviour was described as a "tongue of reversed flow". **Carr et al**[27] also determined that the occurrence of surface flow reversals over the rear portion of the aerofoil are not necessarily equivalent to flow breakdown outside the boundary layer. The investigations by **Seto**[28] and **Niven**[21] on the NACA 23012 and NACA 23012A aerofoils respectively indicated that flow reversals may penetrate upstream to the 30% chord region prior to vortex formation.

These observations raise the question of whether such flow reversals are a prerequisite to vortex inception, and, if so, whether their behaviour is dependent on the aerofoil's steady trailing-edge separation characteristics. One method of investigating this phenomenon was thought to be by correlating the the incidence at which vortex initiation is observed against a designated parameter representing the aerofoil's steady trailing edge characteristics. The results of **McCroskey et al**[26] imply that the incidence at which dynamic stall onset occurs is related to the abruptness of the aerofoil's steady trailing-edge separation. A parameter describing this behaviour was therefore sought.

An approximation to the location of boundary-layer separation at any angle of attack for an aerofoil experiencing trailing-edge separation has been described by **Beddoes**[29]. The variation of the separation point with angle of attack was modelled by two exponential equations which coincided at the 70% chord location. These equations could not accurately model all types of separation

characteristics, such as those typical of the sudden stall possessed by the NACA 23012. They were therefore generalised[16] to the form

$$f = f_{max} + K_1 \exp((\alpha-\alpha_1)/S_1), \quad \alpha \leq \alpha_1 \qquad (2a)$$

$$f = f_{min} + K_2 \exp((\alpha_1-\alpha)/S_2), \quad \alpha > \alpha_1, \qquad (2b)$$

where α represents the angle of attack and **f** represents the separation point in the form of **x/c**, the ratio of the distance from the leading edge to the length of the chord. The remaining seven coefficients are constant for a particular aerofoil and Reynolds number in steady conditions. An algorithm for approximating these constants for any set of data points $\{(\alpha,f)\}$ has been coded[16] and the resulting separation curves for the seven aerofoils illustrated in **Figure 15** are plotted in **Figure 16**. At the time of deriving this correlation, these were the only seven aerofoils which had been tested.

The larger range of values for **f**, including the range of the more sudden forward movement of the separation point, is included in **Equation 2b**. It follows that, at this part of the separation process,

$$df/d\alpha = -S_2^{-1} K_2 \exp((\alpha_1-\alpha)/S_2)$$

$$= -S_2^{-1}(f-f_{min}).$$

The constant f_{min} represents the location of bluff body separation, and is approximately equal for each aerofoil ($0<f_{min}<0.0025$). Therefore, for any given value of **f** in the range of abrupt separation and, in particular, at the 50% chord location which **Scruggs et al**[23] examined when comparing aerofoils' separation characteristics, the rate of change of separation point with respect to incidence is approximately proportional to S_2^{-1}. This argument indicates that the statically-derived coefficient S_2 would be a suitable parameter to use when examining the influence of trailing-edge separation on vortex inception. As a result, it should be possible, in the light of what has been discssed above, to use this parameter when representing, in the form of a single equation for all seven arofoils, the incidence of the earliest indication from experimental ramp data that stall onset has occurred.

In the fully dynamic stall regime, as illustrated in **Figures 12** and **17**, the incidence of C_p deviation α_{ds} varied linearly with reduced pitch-rate **r**. Therefore this relationship can be expressed in the form

$$\alpha_{ds} = m_1 r + c_1, \qquad (3)$$

where m_1 and c_1 represent constants for a particular aerofoil. If the rate of separation influences the formation of the vortex, then it is possible that

$$m_1 = F_1(S_2) m_2,$$

where m_2 is a constant for all aerofoils and $F_1(S_2)$ is a function of S_2 and, hence, of aerofoil. By correlating m_1 against S_2, and with the intention that the function should be as simple as possible, it was decided that $F_1(S_2)$ should be of the form S_2^i, where **i** is a constant for all aerofoils.

Because the steady stall characteristic can be regarded as the characteristic of a ramp at zero pitch-rate, it seemed natural to consider the steady stall incidence α_{ss} as the parameter for determining the offset value c_1 in **Equation 3**. Regardless of how the steady stall angle is defined, correlation of c_1 against α_{ss} indicated that the substitution should be

$$c_1 = c_2 \alpha_{ss} + c_3,$$

where c_2 and c_3 are constants for all aerofoils.

It follows that α_{ds} can be represented in the form

$$\alpha_{ds} = A + B.\alpha_{ss} + C.S_2^i r, \qquad (4)$$

and values for **A**, **B** and **C** must be calculated. Fot this purpose, an algorithm was coded to perform least-squares linear regression in two variables on the data points at a Reynolds number of approximately 1.5×10^6. These two variables were $S_2^i r$ and α_{ss}. For a given value of **i**, the

algorithm calculated **A**, **B**, **C** and the least-squares error. Repeating the process with different values of **i** and comparing the resulting error values provided a suitable equation. Analysis of the data revealed that the most accurate correlation was yielded when **i** was assigned the value of 1/4 and α_{ss} was regarded as the incidence of pitching-moment break in steady conditions.

Only data in the dynamic regime were modelled by **Equation 4**. In order to include the data points which resulted from quasi-static experiments, where the first observed indication of stall was a drop in suction from its maximum magnitude at the leading edge, the original program was modified to include a square-root term. This was a simple and accurate modification, resulting in an equation of the form

$$\alpha_{ds} = A + B.\alpha_{ss} + C.S_2{}^{i}r + (D.S_2{}^{i}r)^{1/2}. \qquad (5)$$

Finally, the correlation was generalised further to include data points recorded over a range of Reynolds numbers. At low Reynolds numbers, the flow is encouraged to separate from the surface at lower angles of attack[13]. It therefore seems plausible that certain aspects of this phenomenon would be extended into unsteady conditions. If vortex inception is influenced by the separation characteristics then it follows that C_p deviation would occur at a lower incidence. Data at the University of Glasgow did reveal that increasing the Reynolds number resulted in an increase in the gradient of the trace of C_p deviation incidence against reduced pitch-rate.

From examination of graphs of various equations, it was observed that the power to which S_2 is raised should be a function of Reynolds number, and that **Equation 5** should be modified to the form

$$\alpha_{ds} = A + B.\alpha_{ss} + C.S_2{}^{Rj}r + (D.S_2{}^{Rj}r)^{1/2}, \qquad (6)$$

where $R = Rex10^{-6}$ and **j** is a constant for all aerofoils. The terms α_{ss} and S_2 were determined at each Reynolds number. The final correlation is illustrated in **Figure 2**. Because **Equation 6** is the equation of a plane in three dimensions, any qualitative comparison of the original set of data points to those predicted by the correlation with the aid of a three-dimensional graph would be very difficult.

Therefore, it was decided to illustrate the correlation by means of a two-dimensional graph ,with the axes labelled $S_2^{Rj}r$ and (α_{ds} - B.α_{ss}). A square-root scale is used on the $S_2^{Rj}r$ axis in order to compare the data in the quasi-static regime more easily.

In **Figure 18**, the correlation is compared with the incidences of C_p deviation recorded for the NACA 23012C aerofoil at a Reynolds number of $1.5x10^6$. In this figure, the correlation is compared to two sets of data points : those determined at 0% chord and at 27% chord. In the quasi-static regime, the incidence at which the local peak suction collapsed at 27% chord is plotted : by the definition described in **Section 3.4**, in the quasi-static regime there was no C_p deviation and so the lowest incidence at which there was a distinct deviation in the pressure coefficient trace at the relevant location in this regime was that at which the gradient of the trace became negative. As would be expected, in the quasi-static regime, the correlation refers to the peak suction collapse at 0% chord and in the dynamic stall regime to the C_p deviation at 27% chord.

McCroskey et al[25] observed that, regardless of behaviour at low Mach number or in the quasi-steady regime, as the freestream Mach number was increased, each aerofoil which they tested tended to exhibit characteristics typical of unsteady leading-edge stall. In such cases, a criterion based on trailing-edge separation may not be justified. It is, therefore, noted that the present correlation is restricted not only to aerofoils which experience trailing-edge separation, but also to test conditions in the low Mach number regime (i.e. freestream Mach numbers of less than 0.2).

This correlation was intended for use when designing aerofoil sections as an indication of an aerofoil's aerodynamic performance in unsteady conditions. It has already been employed[30] to assist in the design of aerofoil sections for both helicopters and vertical-axis wind-turbines.

3.7 Comparison of Correlation with that from Various Modelling Algorithms

Ths section compares the incidence of stall onset as predicted by stall criteria which have been defined by other researchers and assesses their ability to predict the incidence of stall onset as revealed by the data recorded at the University of Glasgow. In **Figure 19**, for the NACA 23012C aerofoil over a range of reduced pitch-rates at a Reynolds number of $1.5x10^6$, each criterion is compared with

the correlation which was derived in **Section 3.6**, stated in **Equation 6** and represented by the "**Cp DEVIATION**" curve.

The models which have been examined are those of :-

(i) **Beddoes et al**[10,14], which is a time-delay model, discussed in **Sections 3.1** and **3.5**, using **Evans and Mort's**[15] correlation in determining dynamic stall onset;

(ii) **Carlson et al**[31], another time-delay model, which proposes that universal time constants exist between the incidences of both moment stall and maximum lift in steady and unsteady conditions;

(iii) **Johnson and Ham**[32], in which the dynamic stall vortex is shed when the laminar separation bubble bursts. It was proposed that the dynamic stall delay results from the delay in the leading-edge bubble reattachment point moving towards the leading-edge and encountering the large adverse pressure gradient;

(iv) **Ericsson and Reding**[33], in which the separation-induced aerodynamic loads are affected by two distinctly different flow phenomena : one of quasi-steady behaviour which is associated with the dynamic delay of flow separation; the other of transient nature associated with the upstream movement of the separation point during dynamic stall and the subsequent spillage downstream of the leading-edge vortex. A time-delay is assocated with each of these phenomena. The dynamic delay of flow separtion is caused by a time-lag (divided further into circulation lag, convective viscous-flow time-lag and moving separation point effect) and boundary-layer improvement effects (split into accelerated flow and moving-wall effects). Of these two effects, the former causes the corresponding static loads to lag the instantaneous flow environment and the latter produces an overshoot of the static stall chararcteristics. There is evidence that the maximum pitch-rate attained during the cycle is important in producing dynamic overshoot of the maximum lift coefficient. It can be seen from **Figure 19** that the gradient of this stall onset trace changes at a reduced pitch-rate of 0.01, which, as descibed in **Section 3.4** was the reduced pitch-rate at which dynamic stall characteristics replaced quasi-static characteristics;

(v) **Gormont**[34], which was developed from the research of **Harris et al**[35]. The force and moment coefficients are constructed from static data using an equivalent angle of attack, which

accounts for unsteady potential flow effects, and a reference angle. In particular, the delay incidence $\Delta\alpha_d$ between static stall and dynamic stall is determined from the equation

$$\Delta\alpha_d = \gamma\sqrt{[(d\alpha/dt)c/U_\infty]},$$

where γ is a function, generated from a large amount of experimental data, of freestream Mach number and the maximum thickness of the aerofoil, and is different for lift and moment stall.

This small selection of stall criteria illustrates the wide variety of stall onset definitions in general use. In all these methods, the y-axis intercept is a function of the steady stall incidence. However, the variation with reduced pitch-rate depends on parameters which vary with model : Beddoes bases his stall incidence on idealised static data based partly on aerofoil geometry with universal time-delays; Carlson et al use a time-delay which is independent of aerofoil and wind-speed; Johnson and Ham's model varies as a function of the steady stall incidence; Ericsson and Reding's parameters were derived from more parameters than any of the other models, but these parameters appear to be constant within various Reynolds number ranges; Gormont's model varies as a function of aerofoil thickness and Mach number. However, as described in **Section 3.6**, correlation of the data at the University of Glasgow required the parameters of Reynolds number and separation characteristics for each aerofoil in steady conditions.

As a consequence of these different criteria, the incidence of stall onset is seen in **Figure 19** to vary greatly. The incidence of C_p deviation was observed to occur amongst the last of the criteria. Of the other criteria, those which appear to define stall onset most closely to C_p deviation are those defined by Gormont and Ericsson and Reding.

It must be stressed that this discussion does not judge the accuracy of these algorithms. The fact that the incidences predicted by some of the algorithms were closer to that of C_p deviation only shows that the mechanism which was required to model aerodynamic behaviour in those cases was closer to that of C_p deviation. Therefore, the wide variation in graphs in **Figure 19** does not indicate differences in accuracy, but, instead, differences in what is required for the specific purposes of each model. For example, the critical angle of **Wilby[36]**, which was always lowest, defines the maximum incidence which can be attained without subsequently incurring full dynamic stall. This incidence

would appear to be of greatest relevance to the research discussed herein. However it can only be determined from data collected during oscillatory pitching motions of the aerofoil. The aim, therefore, was to relate this critical angle to a stall criterion which is easily detectable from purely experimental data under any type of motion (i.e. C_p deviation).

3.8 The Extension of the Correlation to Oscillatory Motion, and a Correlation for an Equivalent Critical Angle of Attack during Ramp Motions

Wilby[36] reasoned that, in oscillatory conditions, aerofoil sections which exhibit the ability to attain high incidence values without experiencing a break in pitching-moment would be beneficial to helicopter rotor performance. In order to calculate the maximum incidence to which an aerofoil could be pitched without moment stall being incurred during the cycle, he examined the data from a series of oscillatory experiments for which the mean angle of attack was increased systemmatically while the amplitude and reduced frequency were fixed. For those tests in which the maximum incidence was sufficiently large for a break in pitching moment to be detected, the difference between the minimum value of pitching-moment coefficient and its unstalled value was calculated. Extrapolating these differences to a value of zero yielded a clearly defined break-point indicating the maximum incidence which could be attained without incurring moment stall. This incidence was termed the critical angle of attack α_c.

It was observed that, like the incidence of C_p deviation, once this angle of attack had been attained, the events of the dynamic stall process could not be reversed. Comparing the incidence of C_p deviation with the critical angle in oscillatory experiments revealed that the critical angle was always attained first. Therefore C_p deviation is not the earliest indication in oscillatory experiments that the stall process has been initiated and cannot be reversed. However, the critical angle can only be determined directly from oscillatory data. For a general type of motion, C_p deviation is the earliest such indication of stall onset that has been observed from these data.

By a similar procedure to that described in **Section 3.6**, an equation was derived to correlate the data for the seven aerofoils illustrated in **Figure 20**. As described in **Section 3.4**, the incidence

of C_p deviation has been observed to be independent of the type of motion when the maximum pitch-rate is considered. It would therefore seem reasonable to use the maximum pitch-rate of a cycle to change the domain of the critical angle correlation from reduced frequency to reduced pitch-rate and so compare the correlations illustrated in **Figures 2** and **20**. In **Figure 19**, these versions of the correlation are compared to each other and the stall criteria discussed in **Section 3.7**. The equivalent critical angle is represented by the **"CRITICAL ANGLE"** curve. It can be seen that it was reached significantly earlier than the incidence of C_p deviation at all pitch-rates. Indeed, by observing the incidences of each of the seven criteria, it can be seen that the critical angle of attack occurred earliest and C_p deviation occurred among the latest of the definitions.

Although based on experimental data, the other five definitions are theoretical and so cannot be detected easily when simply observing the data. It was hoped, when analysing ramp data, to be able to locate the lowest incidence at which the stall process had been initiated and the effects could not be reversed. As the critical angle is the lowest such incidence which has been detected from oscillatory experiments during the present research, it was hoped to locate an incidence which was analogous to the critical angle in ramps. This was not possible from simple observation of the data because, unlike during oscillatory experiments, ramps take place at a constant pitch-rate and, hence, no change in pitch direction could be made when below the stall incidence. However, it is possible to relate theoretically the two definitions described above.

In the dynamic stall regime, the variation of these incidences with reduced pitch-rate is approximately linear. In these cases, the incidence α_{ds} of C_p deviation is given by

$$\alpha_{ds} = 0.152 + 1.210\alpha_{ss} + 243.991S_2^{R/6}r,$$

and the critical angle α_c by

$$\alpha_c = 7.389 + 0.487\alpha_{ss} + 20.188S_2^{R/6}k$$

or

$$\alpha_c = 7.389 + 0.487\alpha_{ss} + 144.586S_2^{R/6}r,$$

where the critical angle correlation has been changed from reduced frequency to reduced pitch-rate by means of the maximum pitch-rate attained during the cycle. Therefore

$$\alpha_{ds} - \alpha_c = (0.723\alpha_{ss} - 7.237) + 99.405S_2^{R/6}r.$$

Now the reduced pitch rate **r** is defined as

$$r := (d\alpha/dt)c/2U_\infty . \pi/180 = (\pi c.\Delta\alpha)/(360U_\infty\Delta t) \qquad (7)$$

for a constant pitch-rate, where $\Delta\alpha$ and Δt can be measured between any two points and where the angle of attack is expressed in degrees. In particular, $\Delta\alpha$ and Δt can be measured between the critical angle and the incidence of C_p deviation and, hence, employing **Equation 7**, the non-dimensional time-delay τ^* can be expressed as

$$\tau^* := \Delta t.U_\infty/c = \pi.\Delta\alpha/360r$$

or

$$\tau^* \approx 0.00631(\alpha_{ss}-10.0)/r + 0.868S_2^{R/6}. \qquad (8)$$

The variation of τ^*, as defined in **Equation 8**, agrees closely with the measured time-delay between these two incidences being attained by the NACA 23012C at a Reynolds number of 1.5×10^6.

3.9 Concluding Remarks

This section has described briefly the most important results of the analysis conducted under the present contract. As well as including a general overview of the aerodynamic characteristics, it has examined aerodynamic damping and various aspects of the events which comprise the dynamic stall process.

From the results of this research and from the data and software which were described in **Section 2**, it has been possible to extend the analysis into areas which were not suggested in the original proposal. A number of these matters are described in the following section.

4 EXTENSION OF RESEARCH BEYOND CONTRACT

4.1 Introduction

This section describes some of the research which was not originally specified as part of the research for this contract, but has grown from, or has only been possible as a result of, the analysis, experiments or procedures which are discussed above. Topics which have benefited from this work have been dynamic stall on both helicopters and vertical-axis wind-turbines, and also blade-vortex interaction.

By liaising with other database users and researchers, routines have been coded and procedures established for recording, transferring, storing and analysing data. As a result, the entire process is now highly efficient and it is very simple to move into new areas of research. This efficiency should continue because all the routines and procedures which are necessary for the entire process have been documented, and this documentation and any relevant software may be accessed by anyone in the research group or authorised user.

4.2 On the Unsteady Re-establishment of Fully-Attached Flow from the Stalled Condition

Although the research for this contract concentrated mainly on the mechanism of dynamic stall onset, a line of research has continued in parallel into the mechanism of reattachment. This research has been performed on all the aerofoils discussed in this report, including the NACA 23012C, but has concentrated on the data from ramps with a constant negative pitch-rate rather than the ramp up tests which were used for examining stall onset. The influence of pitch-rate on the reattachment process has been discussed in detail by **Seto**[28]. **Niven et al**[37] observed from ramp down data for a number of aerofoils that reattachment appeared to move downstream only after the suction at 2.5% chord began to rise, the incidence of which depended on aerofoil geometry, but not on reduced pitch-rate. At reduced pitch-rates of small magnitude, there was a weak dependence on aerofoil motion of the time-delay between the rise in suction and the establishment of fully-attached flow over the aerofoil's upper surface, but at reduced pitch-rates greater in magnitude than 0.015 there was a

constant non-dimensional time-delay of approximately 5 chordlengths of travel. The rate at which the reattachment point moves downstream appears to be independent of the aerofoil geometry.

Of particular interest was the fact that there were regions of negative lift at positive incidences. In order to investigate whether this phenomenon was a result of tunnel interference effects or a valid two-dimensional characteristic of two-dimensional flow, **Niven and Galbraith**[2] conducted a large number of tests in which starting and stopping incidences as well as aspect ratio were varied. It was concluded that a simple estimation of any error in geometrical incidence, induced by the confined flow separation, could not account for the negative normal force at positive geometrical incidences. Instead, prior to any significant leading-edge reattachment, the normal force was dominated by the lower surface pressure distribution which was governed by the aerofoil geometry and the instantaneous flow incidence.

4.3 Current Use of the Incipient-Stall Correlation in Wind-Energy Research

When discussing aspects of the power regulation of vertical-axis wind-turbine machines by the dynamic stall process, **Galbraith and Coton**[38] concluded that VAWT blades can be aerodynamically tailored to utilise the stall phenomenon. As a result, it is possible to influence fatigue loadings and, hence, turbine life. It was proposed that the resulting blades could, in the first instance, possess variation of the aerofoil section along the span and moderate taper, but that further investigation would be required before a reasonable speculation on twist could be made. In order to come to these conclusions, it was necessary to apply the dynamic stall correlation (discussed in **Section 3.6**) and the generalised version of the code for determining the exponential form of trailing-edge separation characteristics (referred to in **Section 3.1** and described by **Gracey**[16]).

With the aid of the University of Glasgow's aerofoil design package, a series of aerofoils was designed by **Jiang and Galbraith**[30] for use on vertical-axis wind-turbines. All of these aerofoils had sharp noses producing a large adverse pressure gradient near the leading edge at medium incidences and result in the separation bubble bursting at a lower angle of attack than those aerofoils with more rounded leading edges. In order to determine which aerofoil to test, the dynamic stall

correlation (discussed in **Section 3.6**) was employed as a guide to how the aerofoil would perform in unsteady conditions. The static characteristics were determined from **Coton's**[39] code. A model of the resulting aerofoil, which was modified from the NACA 0018 aerofoil and illustrated in **Figure 20**, has been built and is currently being tested in the manner of the aerofoils discussed in this report.

4.4 Further Work on the Stall-vortex Convection-speed

The observed timing of dynamic stall events was described in **Section 3.5**. Part of this description revealed that the dynamic stall vortex was shed downstream at a rate which was independent of aerofoil motion. When widening their analysis to the entire database this behaviour was supported by **Green et al**[22,40], who also compared[41] these results to those of **Lorber and Carta**[42]. They observed that, although there were strong similarities in the trends exhibited by the aerodynamic coefficients, there were significant differences between the two sets of data. In particular, Lorber and Carta observed that the vortex velocity increased linearly with reduced pitch-rate. There are also differences in the aerodynamic coefficients.

It was thought that these differences may result from differences between test conditions. The only significant differences were the model aspect ratio and tunnel blockage. Therefore, a model of the NACA 0015 with a chord of length 0.275m was built and tested. When installed in the Handley-Page wind-tunnel, this model had an aspect ratio and blockage ratio superior to Lorber and Carta's test configuration. The data yielded by these tests are now being analysed.

4.5 Analysis of Blade-Vortex Interaction Data

Analysis has been performed by **Horner et al**[43,44,45] on the data, recorded during blade-vortex interaction tests, which were transferred as described in **Section 2.2**. Detailed pressure measurements taken about the surface of the aerofoil during parallel interaction with a free vortex showed that the development and collapse of the leading-edge suction peak, together with evidence of

propagative and convective disturbances associated with the overhead passage of the vortex. The integration of normal, tangential and pitching-moment coefficients revealed force and moment behaviour was linked to vortex position. The effect of vortex-leading edge and vortex-trailing edge interation was evident. The effect of the overhead passage of a vortex-associated diturbance was relatively small in force and pressure data, but it profoundly effected the pitching-moment data.

The pressure histories which were examined exhibited the same response to changes in vortex-induced incidence which had previously been noted in both experimental and computational blade-vortex interaction studies. In particular, many of the features which have been observed or measured at the University of Glasgow were predicted by **Lee and Smith**[46].

The data which were collected during parallel and oblique interactions were compared. It was observed that there existed many qualitative and quantitative similarities, such as the rise and collapse of the leading-edge suction, the convective disturbances associated with the close overhead passage of the interaction vortex and the gross features of the integrated airloads. However, there were also differences which, although slight, highlighted the three-dimensional nature of the flows generated during blade-vortex interactions. These flows yielded largely different effects depending on whether tests were conducted in the second or third azimuthal quadrant, suggesting that, in full rotor tests, similar variations might arise depending on whether interacting vortices were inclined towards the root or the tip of the rotor blade.

A correlation of vortex position with perturbations in the coefficients of pressure, normal force and pitching-moment were observed. This led to an association of vortex trailing-edge passage with particularly strong perturbations in force and moment data. The magnitudes of the peaks, valleys and perturbations of all data were strongly dependent on the non-dimensional vortex strength used during the tests. This was particularly true for the maximum value of normal force coefficient.

The nature of the perturbations in force and moment data during the overhead passage of the vortex was found to differ greatly depending on which side of the aerofoil the vortex passed. In the case of "head-on" interactions, it was suggested from pressure, force and moment data that the vortex was split into two fragments, each passing over opposite sides of the aerofoil. In all cases the perturbations in these data were consistent with the expected consequences of passing a low-pressure vortex close to an aerofoil.

In examining vortex passage, it was observed that vortex/blade separation heights strongly influenced separation velocities. It was particularly evident that the vortex convected more rapidly over the aerofoil upper surface, and more slowly over the lower surface.

5 FUTURE PROSPECTS

5.1 INTRODUCTION

As was mentioned earlier, the work described herein forms part of a larger activity that is continuing. The purpose of the present section is to give an indication of the major interests which we hope to pursue in the coming years.

5.2 Roughness transition strips on models

Whilst assessing the effects of tunnel constraints upon the Glasgow University facility we tested a model with half the chord length of that which we normally consider. This brought the overall geometric conditions within the tunnel to be in line with those of **Lorber and Carta**[42] whose measured data showed identifiable inconsistencies with those from Glasgow. The reduced chord length resulted in a correspondingly reduced Reynolds number and data that was difficult to interpret. In addition to our normal tests we decided to trip the boundary layer in the region of the leading edge by a suitable deposition of graded sand. This gave a significant change in the measurements and this was especially noticeable in the pseudo three-dimensional plots illustrating the time histories of the pressure profile (**Figure 22**). These changes gave a corresponding marked alteration to the assessment of the dynamic stall vortex convection speed (**Figure 23**). This is currently receiving much investigation and a large chord model with a suitable trip has just completed an appropriate test programme.

5.3 Three-dimensional dynamic stall

Almost all the dynamic stall assessment codes used in rotorcraft performance work are nominally two-dimensional. In the region of the rotor tip the flow is three-dimensional and so current and readily available assessment codes cannot accurately or satisfactorily assess the flow in that region. In particular, modern rotor blades possess three-dimensional geometries at the tip and this is particulary noticeable in the U.K. BERP tip which helped Westland Helicopters obtain the world speed record. Three-dimensional codes are being developed, but to date there has been only one restricted set of tests conducted, the data from which may be used for code validation. It is hoped in the near

future to develop our established nominally two-dimensional dynamic stall facilities to have a three-dimensional stall capability. Not only will this provide data for the description of such flow phenomena, leading to better formulated assessment codes, but also sought after validation data. It is hoped that such work will assist in maintaining the United Kingdom at the forefront of this particular technology and aid the development of quieter helicopter rotors.

5.4 Discrete vortex algorithms

Dynamic Stall is a highly non-linear phenomenon which has been extensively investigated in the restricted environment of wind tunnels of varying shapes and sizes. The collected data are often used to improve or even develop assessment codes to be used in performance calculations of real rotors. Seldom has there been any consideration of the constraints imposed upon such tests by the constricted environment of the wind tunnel. We hope that discret vortex methods, in which the flow environment for both the wind tunnel and free air can be modelled, will be beneficial towards gaining an appreciation of tunnel constraints. Additionally the discrete vortex techniques, with suitable empirical inputs, can aid not only the understanding of the flow details but also provide justification for interpretations of measured data.

5.5 Particle Image Velocimetry prospects

Flow visualisation is normally carried out at very low Reynolds numbers. This is particularly so if the flow medium is air with a suitable visible contaminant introduced at suitable locations. The Reynolds numbers effects can be significant, as may be gleaned from section 5.2 above. Partical Image Velocimetry techniques can eleviate this problem by deducing the velocity vectors at particular locations from the speckle pattern of light reflected from dust particles over an accurately timed interval. At any instant a two-dimensional slice of a flow field can be obtained and, from the velocity field, the corresponding vorticity field may be obtained. This technique will undoubtedly be of benefit to the interpretation of measured pressure data and aid the resolution of anomolies associated with the ramp down motions mentioned in previous sections.

6 CONCLUDING REMARKS

All of the research which was proposed in this contract has not only been completed but also extended. There has been development and documentation of techniques by which data can be transferred and stored quickly and efficiently on the University of Glasgow's aerofoil database. The data can then be analysed almost immediately.

The analysis described above has looked at general aerodynamic characteristics in both steady and unsteady conditions, and has then examined particular behaviour of these characteristics in greater detail. These areas have included aerodynamic damping, vortex inception and the timing of dynamic stall events. A correlation between the earliest incidence which can be observed from general motion that the dynamic stall vortex has been initiated and an aerofoil's steady characteristics has been derived, and this has been compared to a number of other criteria for stall onset. It has been possible to correlate all types of aerofoil motion by means of the maximum attained pitch-rate, and, through this, to define an earlier incidence, analogous to the critical angle in oscillatory conditions, which is independent of motion type. Thus unsteady aerodynamic characteristics can be examined purely from ramps, for which a much wider range of test conditions is possible.

The research has been extended beyond the contract proposals to include unsteady flow reattachment, the design of vertical-axis wind-turbines, a comparison of the timing of dynamic stall events with data from outside the University of Glasgow, and blade-vortex interaction.

7 ACKNOWLEDGEMENTS

The authors wish to acknowledge the encouragement and support of their colleagues both academic and technical. In particular they thank Dr F.N.Coton, Dr R.B.Green, Mr M.B.Horner, Dr Jiang Dachun and Dr A.J.Niven for their contribution to the research discussed herein. The backing and support of Westland Helicopters, in particular Mr T. S. Beddoes, and VAWT Ltd, in particular Mr A. Harris, is also greatly appreciated.

8 REFERENCES

[1]**Angell, R.K., Musgrove, P. J., Galbraith, R.A.McD. and Green, R. B.** Summary of the collected data for tests on the NACA 0015, NACA 0018, NACA 0021, NACA 0025 and NACA 0030 aerofoils. Glasgow University Aero Report 9005, February 1990.

[2]**Niven, A.J. and Galbraith, R.A.McD.** Experiments on the establishment of fully attached aerofoil flow from the fully stalled condition during ramp-down motions. 17th ICAS Conference, Stockholm, Sweden, 1990.

[3]**Coton, F.N. and Galbraith, R.A.McD.** An aerofoil design methodology for low speed aerofoils. 10th Annual Wind Energy Conference, London 1988.

[4]**Gracey, M.W. and Galbraith, R.A.McD.** Data for a NACA 23012C aerofoil pitched about its quarter chord axis. Volume I : Pressure data from static and ramp function tests, with photographs of oil-flow visualisation tests. Glasgow University Aero Report 8901, January 1989.

[5]**Gracey, M.W. and Galbraith, R.A.McD.** Data for a NACA 23012C aerofoil pitched about its quarter chord axis. Volume II : Pressure data from oscillatory tests. Glasgow University Aero Report 8902, January 1981.

[6]**Angell, R.K., Musgrove, P.J. and Galbraith, R.A.McD.** Collected data for tests on a NACA 0021 aerofoil. Volume III : Pressure data relevant to the study of large scale vertical axis wind turbines. Glasgow University Aero Report 8802, June 1988.

[7]**Niven, A.J. and Galbraith, R.A.McD.** A user guide to the Beddoes model. Glasgow University Aero Report 9105, May 1991.

[8]**Basuno, B., Coton, F.N. and Galbraith, R.A.McD.** On the aerodynamic modelling of V.A.W.T. Invited lecture at IMECHE H.Q., 23 November 1990.

[9]**Basuno, B., Coton, F.N. and Galbraith, R.A.McD.** A prescribed wake model for vertical axis wind turbines. Submitted to the Journal of the Institute of Mechanical Engineers.

[10]**Leishman, J.G. and Beddoes, T.S.** A semi-empirical model for dynamic stall. Journal of the American Helicopter Society, Volume 34, Number 3, July 1989.

[11]**Leishman, J.G.** Validation of approximate indicial functions for two-dimensional subsonic compressible flow. University of Maryland Report UM-AERO-87, February 1987.

[12]**Leishman, J.G.** Practical modelling of unsteady aerofoil behaviour in nominally attached two-dimensional compressible flow. University of Maryland Report UM-AERO-87-6, April 1987.

[13]**Leishman, J.G. and Beddoes, T.S.** A semi-empirical model for dynamic stall. University of Maryland Report UM-AERO-87-24, July 1987.

[14]**Beddoes, T.S.** Onset of leading edge separation effects under dynamic conditions and low Mach number. 34th Annual National Forum of the American Helicopter Society, Washington D.C., May 1978.

[15]**Evans, W.T. and Mort, K.W.** Analysis of computed flow separation parameters for a set of sudden stalls in low speed two-dimensional flow. NASA Technical Note D-85, 1959.

[16]**Gracey, M.W.** The design and low Mach number wind-tunnel performance of a modified NACA 23012 aerofoil, with an investigation of dynamic stall onset. Glasgow University Aero Report 9108, June 1981.

[17]**McCroskey, W.J.** The phenomenon of dynamic stall. Von Karman Institute for Fluid Dynamics Lecture Series 1981-4 : Unsteady airloads and aeroelastic problems in separated and transonic flow, March 1981.

[18]**Dadone, L.** Rotor airfoil optimization : an understanding of the physical limits. 34th National Forum of the American Helicopter Society, Washington D.C., May 1978.

[19]**Gracey, M.W., Niven, A.J. and Galbraith, R.A.McD.** A consideration of low speed dynamic stall onset. 15th European Rotorcraft Forum, Paper Number 11, Amsterdam, September 1989.

[20]**Seto, L.Y. and Galbraith, R.A.McD.** The effect of pitch-rate on the dynamic stall of a NACA 23012 aerofoil. 11th European Rotorcraft Forum, Paper Number 34, London, September 1985.

[21]**Niven, A.J.** An experimental investigation into the influence of trailing-edge separation on an aerofoil's dynamic stall performance. Glasgow University Aero Report 9107, September 1988.

[22]**Green, R.B., Galbraith, R.A.McD. and Niven, A.J.** Measurements of the dynamic stall vortex convection speed. 17th European Rotorcraft Forum, Paper Number 91-68, Berlin, September 1991.

[23]**Scruggs, L.Y., Nash, J.F. and Singleton, R.E.** Analysis of dynamic stall using unsteady boundary layer theory. NASA Report CR-2462, October 1974.

[24]**McAlister, K.W. and Carr, L.W.** Dynamic stall experiments on the NACA 0012 aerofoil. NASA Technical Paper 1100, January 1978.

[25]**McCroskey, W.J., McAlister, K.W., Carr, L.W., Pucci, S.L., Lambert, O. and Indergand, R.F.** Dynamic stall on advanced aerofoil sections. Journal of the American Helicopter Society, Volume 13, Number 1, pp 40-50, January 1981.

[26]**McCroskey, W.J., Carr, L.W. and McAlister, K.W.** Dynamic stall experiments on oscillating aerofoils. AIAA Journal, Volume 14, Number 1, pp 57-63, January 1976.

[27]**Carr, L.W., McAlister, K.W. and McCroskey, W.J.** Analysis of the development of dynamic stall based on oscillating airfoil experiments. NASA Technical Note D-8382, January 1977.

[28]**Seto, L.Y.** An experimental investigation of low speed dynamic stall and reattachment of the NACA 23012 aerofoil under constant pitch motion. Glasgow University Aero Report 8829, August 1988.

[29]**Beddoes, T.S.** Representation of airfoil behaviour. Vertica, Volume 7, Number 2, pp 183-197, 1983.

[30]**Jiang Dachun and Galbraith, R.A.McD.** A new test aerofoil section for vertical axis wind turbines. Glasgow University Aero Report 9012, March 1990.

[31]**Carlson, R.G., Blackwell, R.H., Commerford, G.L. and Mirick, P.H.** Dynamic stall modeling and correlation with experimental data on airfoils and rotors. Paper Number 2, NASA SP-352, 1974.

[32]**Johnson, W. and Ham, N.D.** On the mechanism of dynamic stall. Journal of the American Helicopter Society, October 1972.

[33]**Ericsson, L.E. and Reding, J.P.** Fluid dynamics of dynamic stall. Part I : Unsteady flow concepts. Journal of Fluids and Structures, Volume 2, pp 1-33, 1988.

[34]**Gormont, R.E.** A mathematical model of unsteady aerodynamics and radial flow for application to helicopter rotors. U.S. Army AMRDL - Eustis Directorate Report TR-72-51, 1972.

[35]**Harris, F.D., Tarzanin, F.J. and Fisher, R.K.** Rotor high speed performance : theory versus test. Journal of the American Helicopter Society, Volume 15, Number 3, July 1970.

[36]**Wilby, P.G.** The aerodynamic characteristics of some new RAE blade sections, and their potential influence on rotor performance. Vertica, Volume 4, pp 121-133, 1980.

[37]**Niven, A.J., Galbraith, R.A.McD. and Herring, D.G.F.** Analysis of reattachment during ramp down tests. Vertica, Volume 13, Number 2, pp 187-196, 1989.

[38]**Galbraith, R.A.McD. and Coton, F.N.** On the passive stall regulation of VAWTs. B.W.E.A. Conference, Norwich, 1990.

[39]**Coton, F.N.** Contributions to the prediction of low Reynolds number aerofoil performance. Glasgow University Aero Report 8818, September 1988.

[40]**Green, R.B., Galbraith, R.A.McD. and Niven, A.J.** Measurements of the dynamic stall vortex convection speed. Glasgow University Aero Report 9014, August 1990.

[41]**Green, R.B., Galbraith, R.A.McD. and Niven, A.J.** The dynamic stall vortex convection speed anomaly : analysis of Lorber and Carta's pressure data. Glasgow University Aero Report 9101, April 1991.

[42]**Lorber, P.F. and Carta, F.O.** Unsteady stall penetration experiments at high Reynolds number. AFOSR TR-87-1203, UTRC Report Number R87-956939-3.

[43]**Horner, M.B., Saliveros, E. and Galbraith, R.A.McD.** An experimental investigation of the oblique blade-vortex interaction. 17th European Rotorcraft Forum, Paper Number 91-62, Berlin, September 1991.

[44]**Horner, M.B., Saliveros, E. and Galbraith, R.A.McD.** An examination of vortex convection effects during blade-vortex interaction. AHS/RAeS International Specialists Meeting on Rotorcraft Acoustics and Rotor Fluid Dynamics, Philadelphia, October 1991.

[45]**Horner, M.B., Saliveros, E., Kokkalis, A. and Galbraith, R.A.McD.** Results from a set of low speed blade-vortex interaction experiments. Submitted to Journal of Experiments in Fluids, September 1991.

[46]**Lee, D.J. and Smith, C.A.** Distortion of the vortex core during blade-vortex interaction. AIAA Paper 87-1243, 1987.

	C_p DEVIATION	MAXIMUM PEAK LEADING-EDGE SUCTION	SHEDDING OF VORTEX FROM 27% CHORD	SHEDDING OF VORTEX FROM TRAILING-EDGE
STATIC STALL	r^{-1}	r	r^{-1}	r
C_p DEVIATION		r	r	r^0
MAXIMUM PEAK LEADING-EDGE SUCTION			r^0	r^0
SHEDDING OF VORTEX FROM 27% CHORD				r^0

TABLE 1 : FUNCTION OF REDUCED PITCH-RATE TO WHICH NON-DIMENSIONAL TIME-DELAY IS PROPORTIONAL

Table lists a series of powers to which **r** *is raised. The non-dimensional time-delay between the event in the left-hand column and that in the top row is, to a first order, proportional to this function of* **r**.

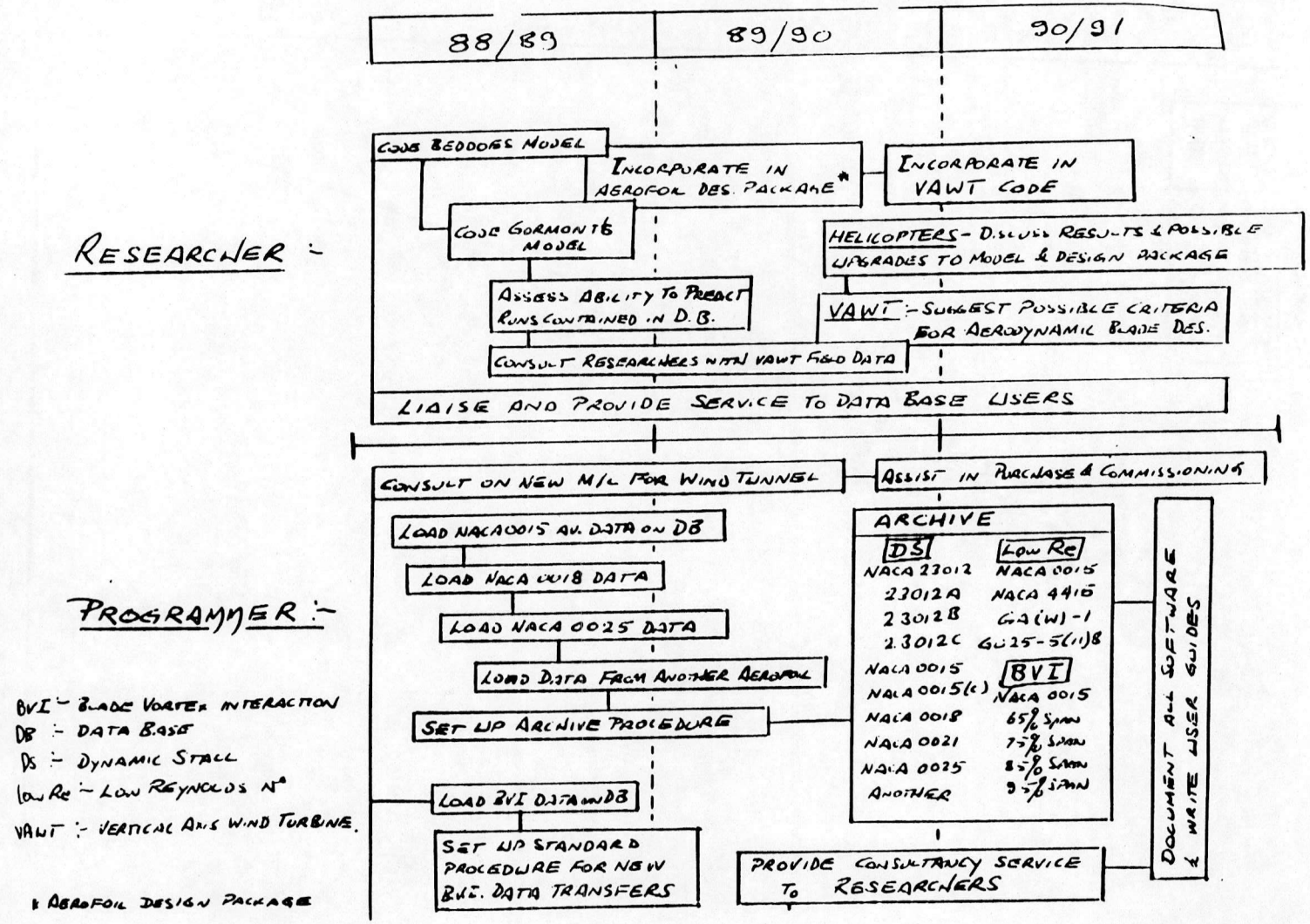

Figure 1 : Proposed work for present contract.

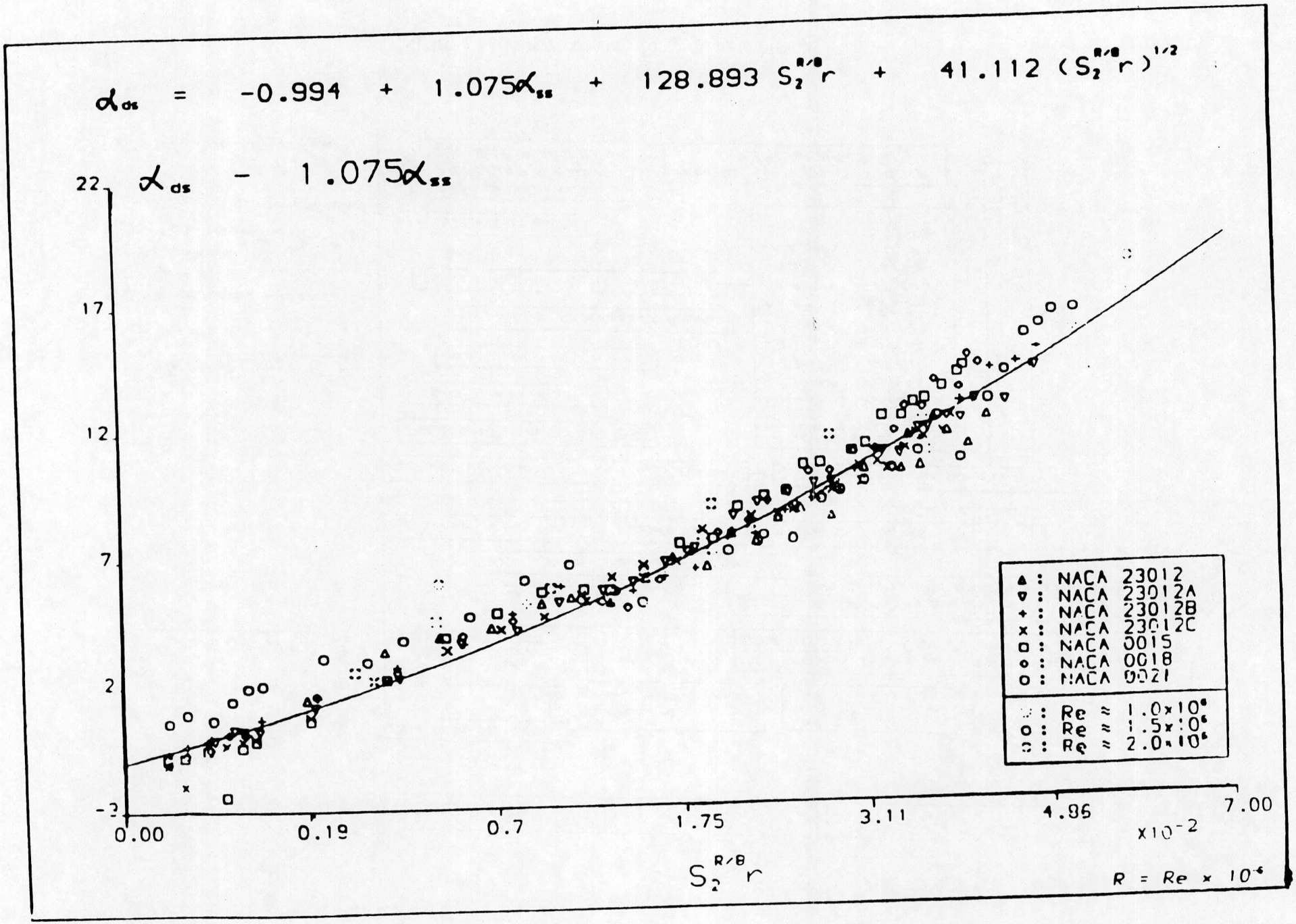

Figure 2 : Correlation of C_p deviation incidences.

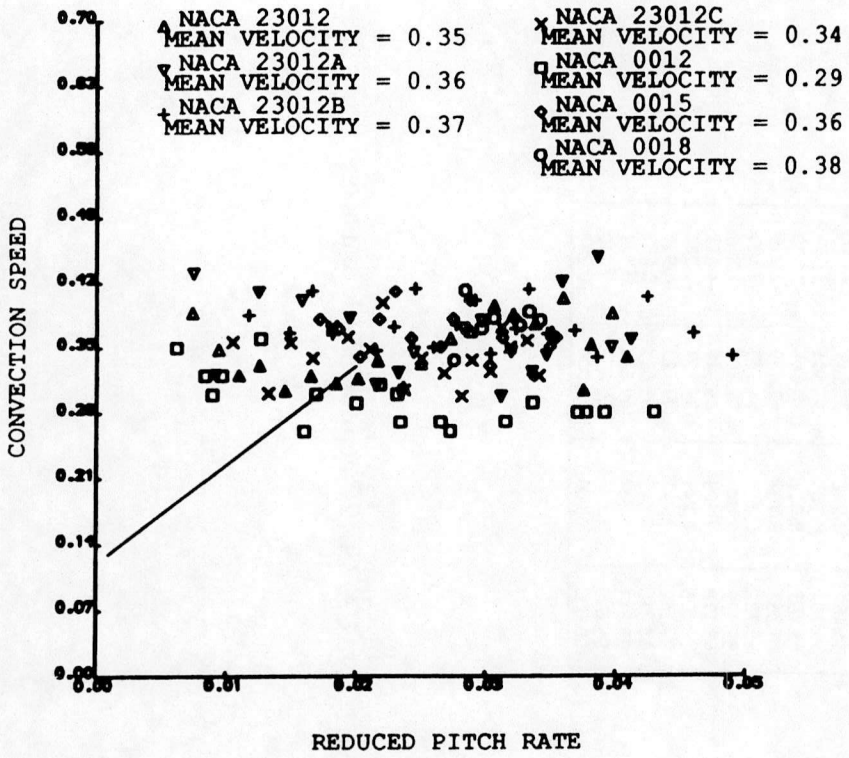

Figure 3 : The collected stall vortex convection speed data for ramp-up motion. Lorber and Carta's result is shown by the solid line.

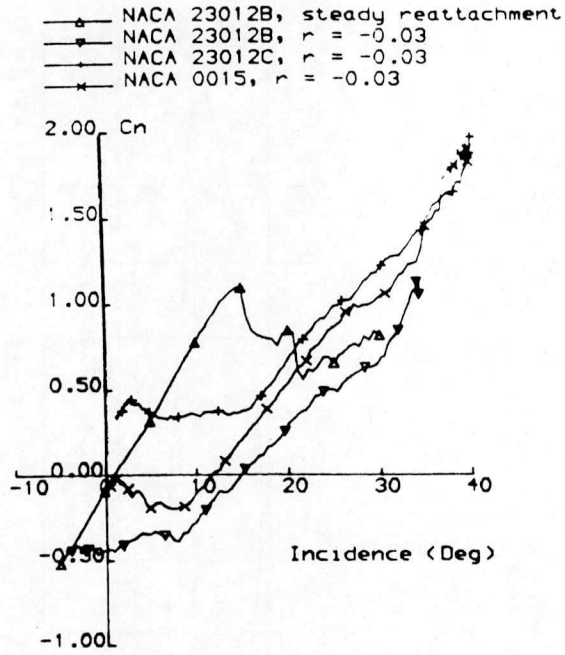

Figure 4 : Normal force behaviour for ramp-down motion.

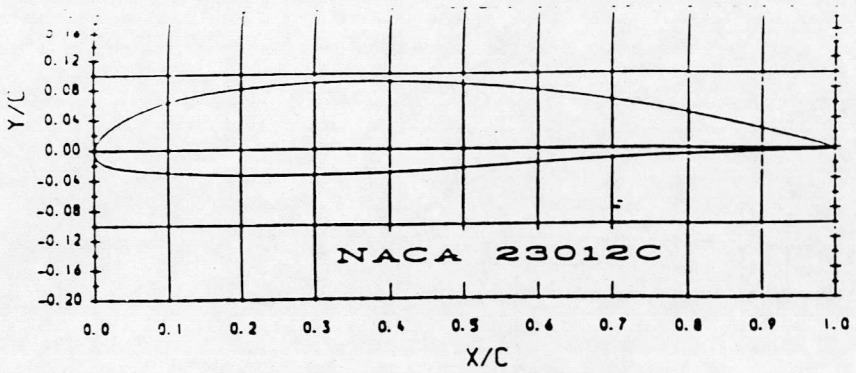

Upper Surface		Lower Surface	
Station	Ordinate	Station	Ordinate
0.000	0.000	0.000	0.000
0.341	0.917	0.657	-1.453
1.124	1.932	1.472	-1.948
2.366	3.009	2.614	-2.310
4.071	4.097	4.064	-2.568
6.232	5.135	5.811	-2.757
8.826	6.072	7.854	-2.905
11.813	6.862	10.206	-3.038
15.139	7.489	12.892	-3.167
18.741	7.965	15.942	-3.291
22.585	8.339	19.393	-3.386
24.873	8.529	23.243	-3.401
29.023	8.783	29.525	-3.345
33.467	8.942	33.969	-3.245
38.184	8.985	38.681	-3.062
43.156	8.914	43.641	-2.830
48.362	8.702	48.829	-2.515
53.782	8.335	54.223	-2.187
59.395	7.803	59.803	-1.857
65.178	7.105	65.546	-1.533
71.108	6.243	71.429	-1.224
77.162	5.222	77.429	-0.931
83.316	4.046	83.523	-0.657
89.547	2.684	89.686	-0.419
95.829	1.136	95.892	-0.340
100.000	0.000	100.000	-0.288

Figure 5 : NACA 23012C aerofoil profile and coordinates.

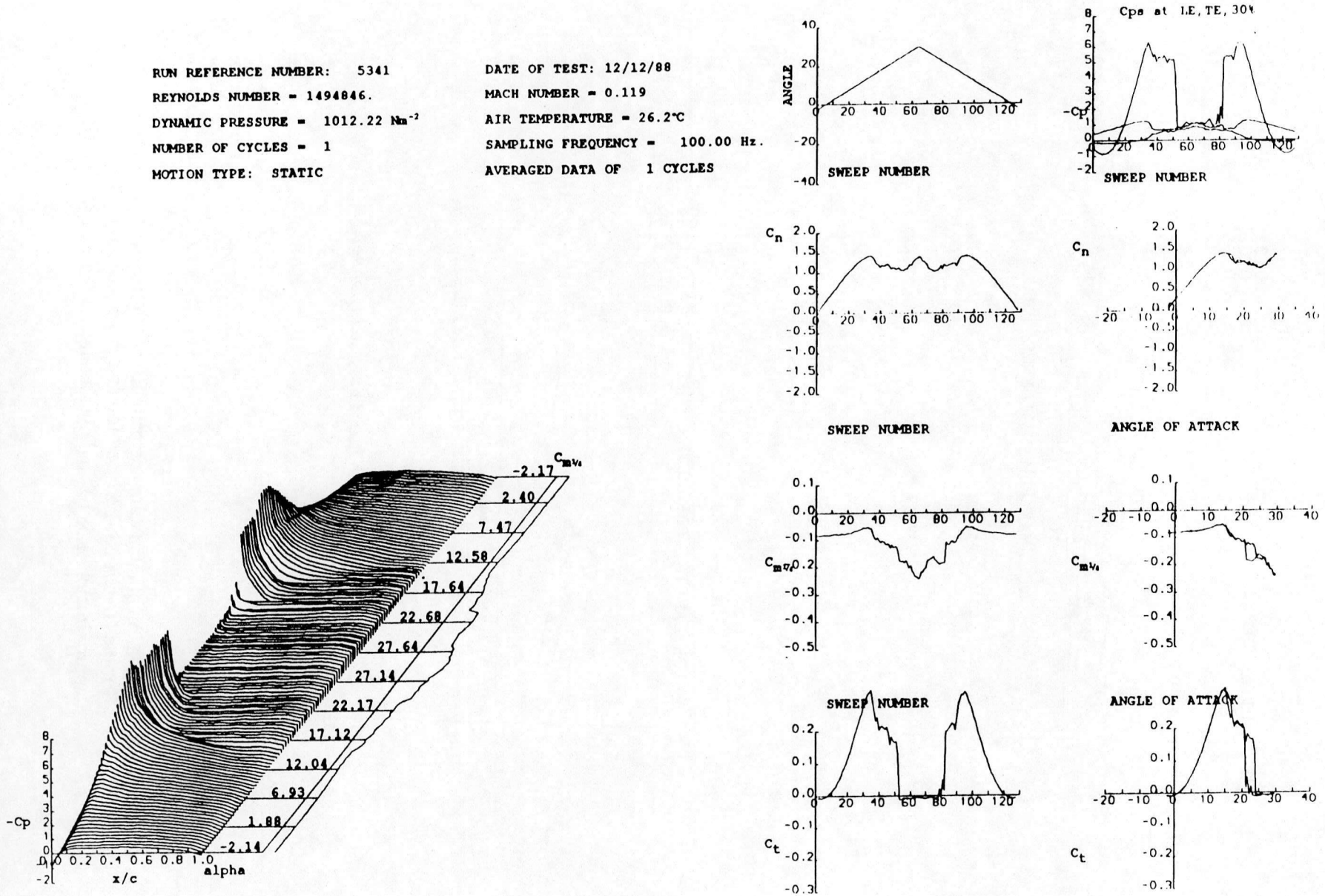

Figure 6: Static characteristics of the NACA 23012C aerofoil at a Reynolds number of approximately 1.5×10^6.

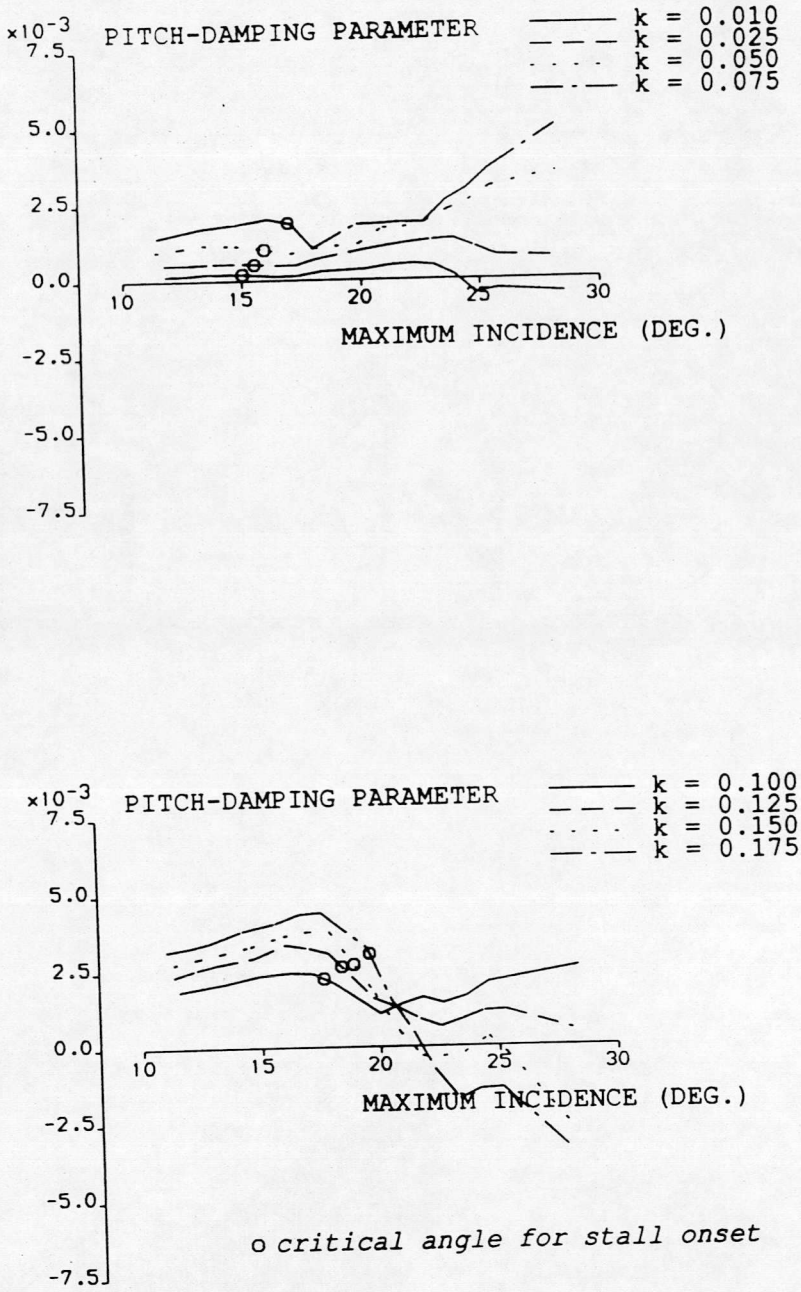

Figure 7 : Variation of pitch-damping parameter with maximum incidence for the NACA 23012C aerofoil at a Reynolds number of approximately 1.5×10^6 and over a range of reduced frequencies.

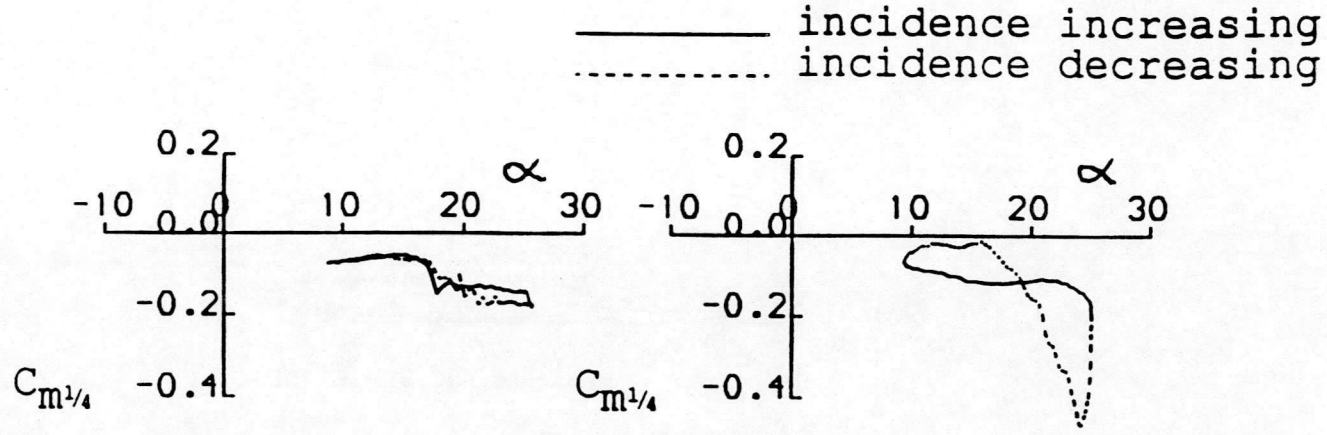

(a) Reduced frequency of 0.010.

(b) Reduced frequency of 0.177.

Figure 8 : Pitching-moment coefficient traces for the NACA 23012C aerofoil at a Reynolds number of approximately 1.5×10^6 and two reduced frequencies.

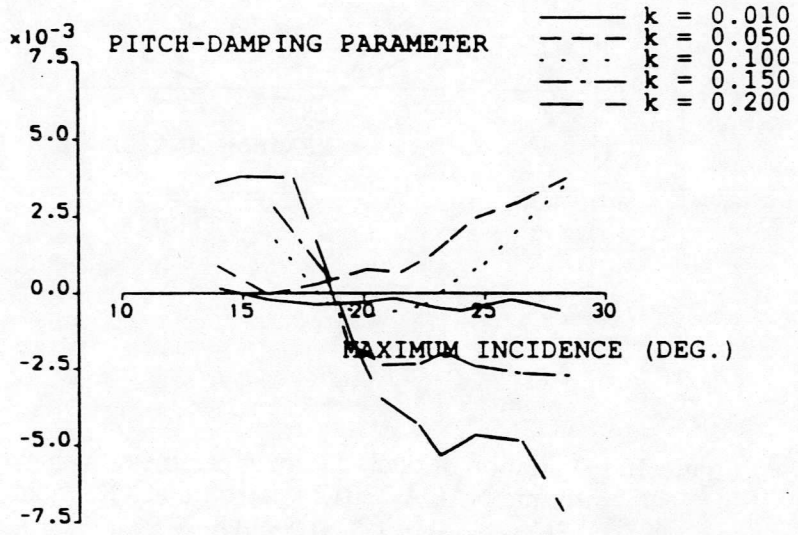

Figure 9 : Variation of pitch-damping parameter with maximum incidence for the NACA 23012 aerofoil at a Reynolds number of approximately 1.5×10^6 and over a range of reduced frequencies.

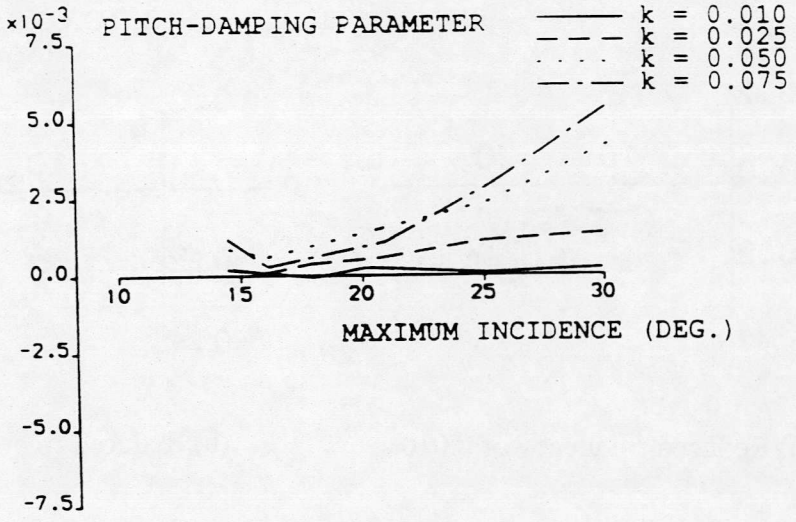

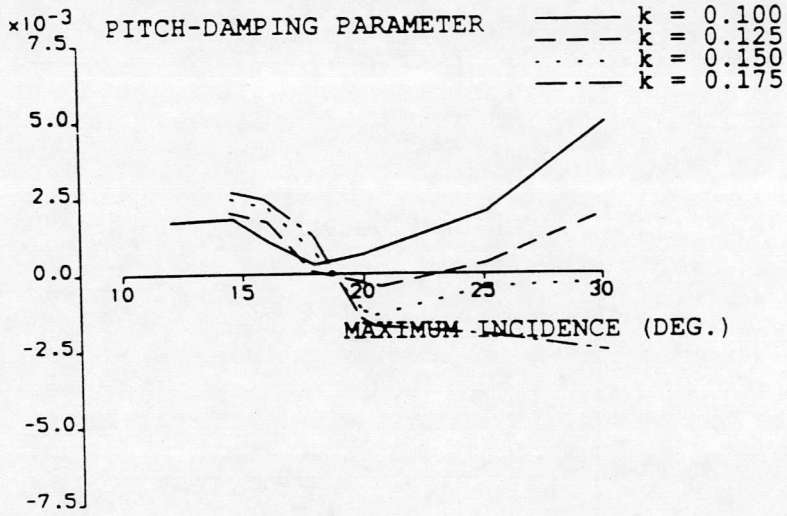

Figure 10 : Variation of pitch-damping parameter with maximum incidence for the NACA 23012A aerofoil at a Reynolds number of approximately 1.5×10^6 and over a range of reduced frequencies.

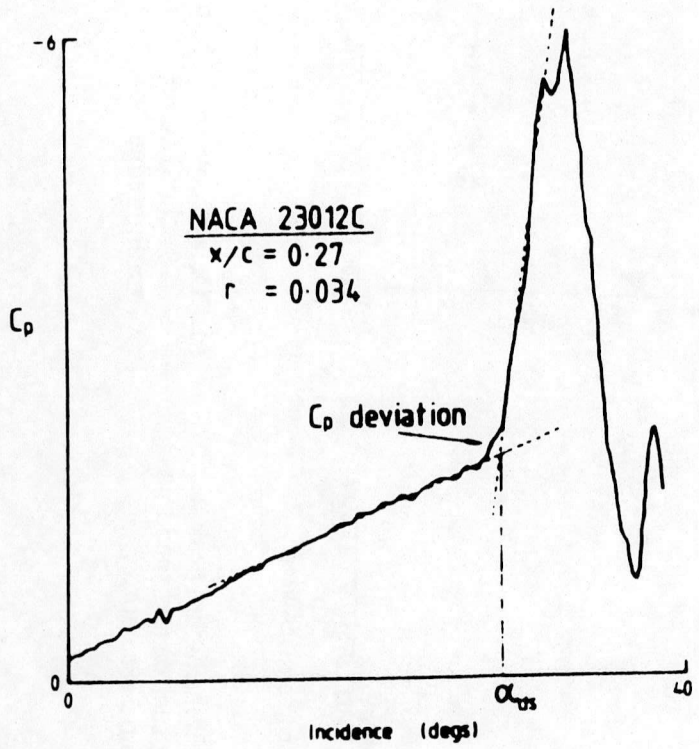

Figure 11 : Defined incidence of dynamic stall onset from pressure trace.

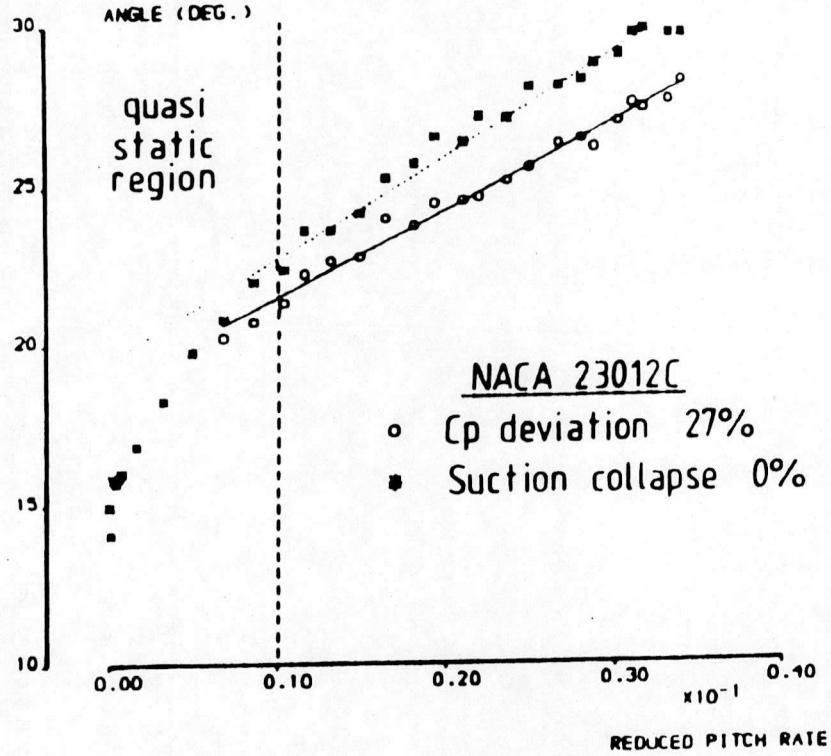

Figure 12 : Variation of defined dynamic stall onset incidence with reduced pitch-rate for the NACA 23012C aerofoil at a Reynolds number of approximately 1.5×10^6.

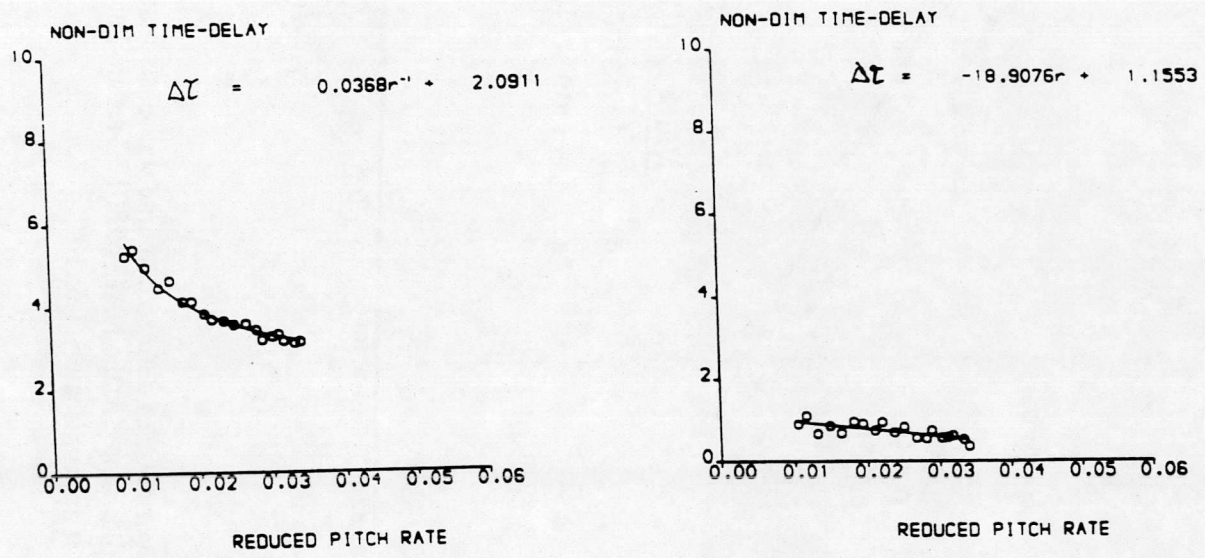

(a) Delay between steady stall incidence and C_p deviation.

(b) Delay between C_p deviation and maximum peak leading-edge suction.

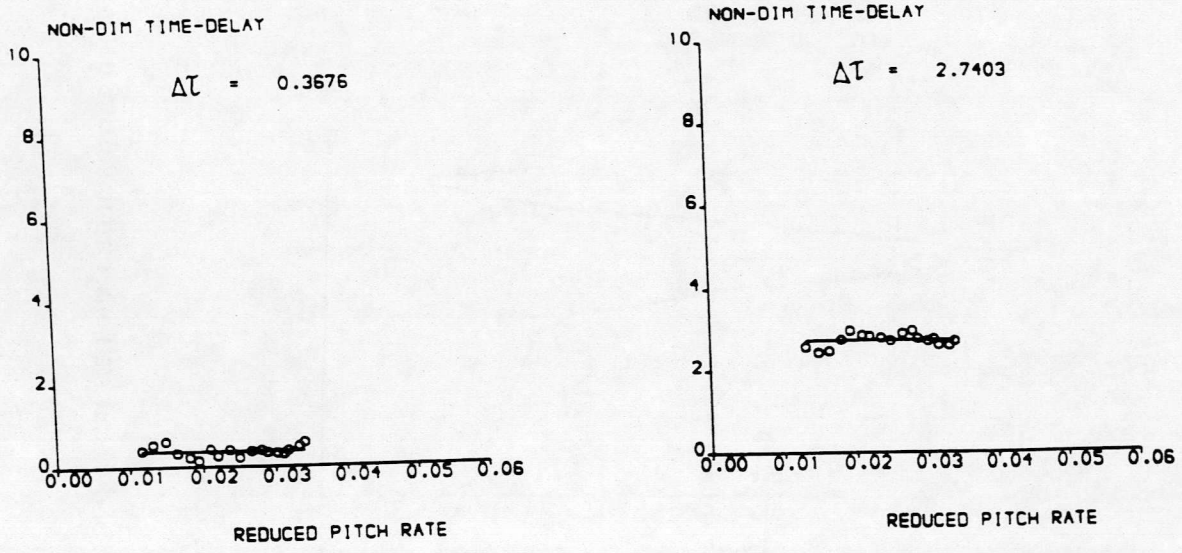

(c) Delay between maximum peak leading-edge suction and shedding of vortex from 27% chord.

(d) Delay between shedding of vortex from 27% chord and releasing of vortex from trailing-edge.

Figure 13 : Variation of various time-delays with reduced pitch-rate for the NACA 23012C aerofoil at a Reynolds number of approximately 1.5×10^6.

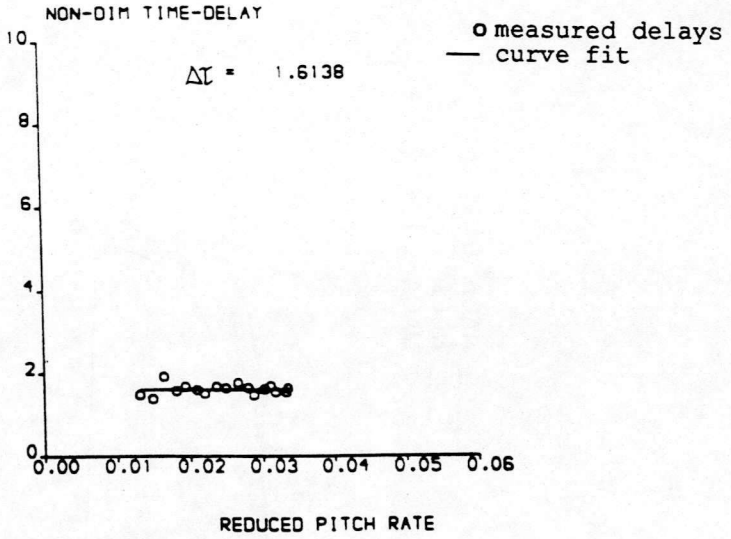

Figure 14 : Variation with reduced pitch-rate of the time delay between Beddoes's definition of dynamic stall onset and C_p deviation for the NACA 23012C aerofoil at a Reynolds number of approximately 1.5×10^6.

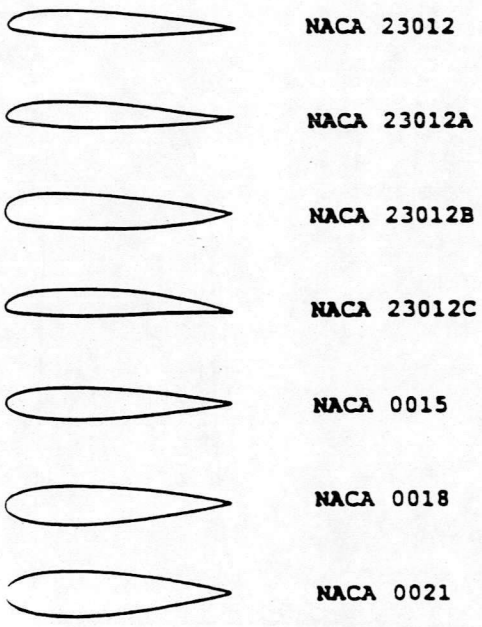

Figure 15 : Seven aerofoils tested at the University of Glasgow.

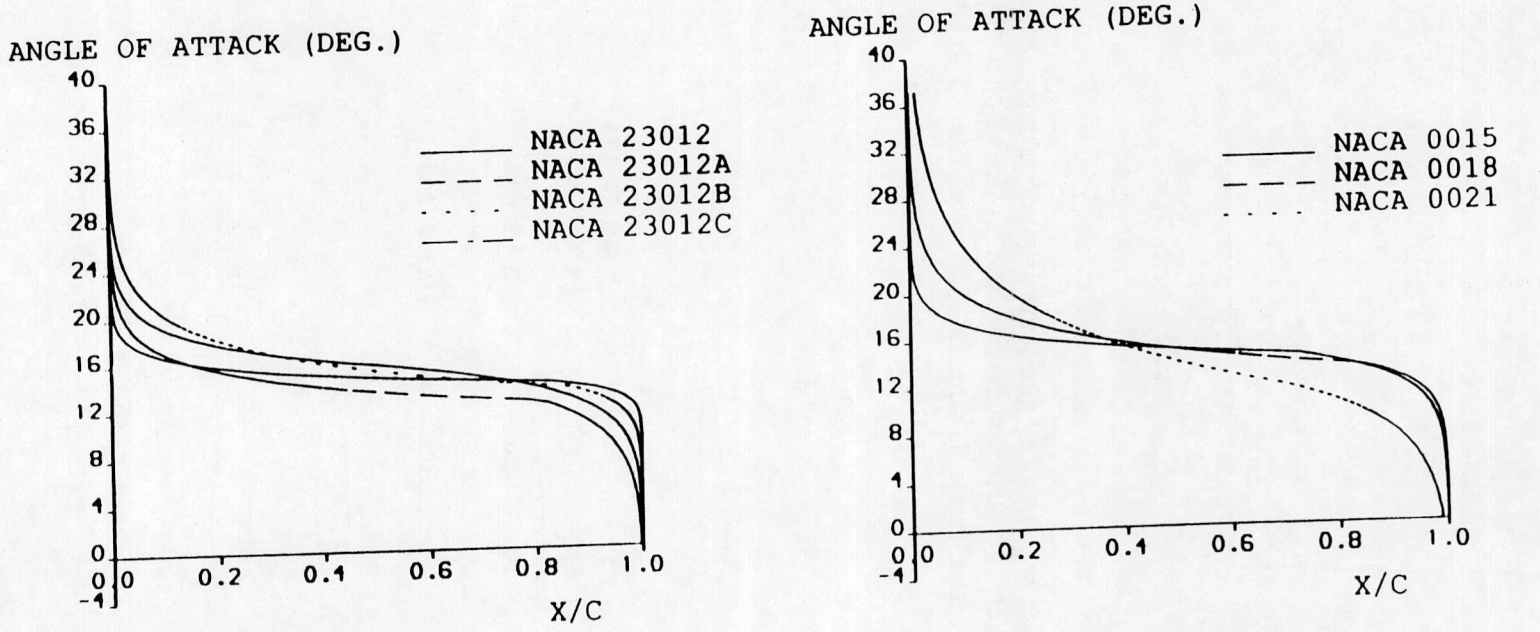

Figure 16 : Steady trailing-edge separation characteristics for seven aerofoils at a Reynolds number of approximately 1.5×10^6.

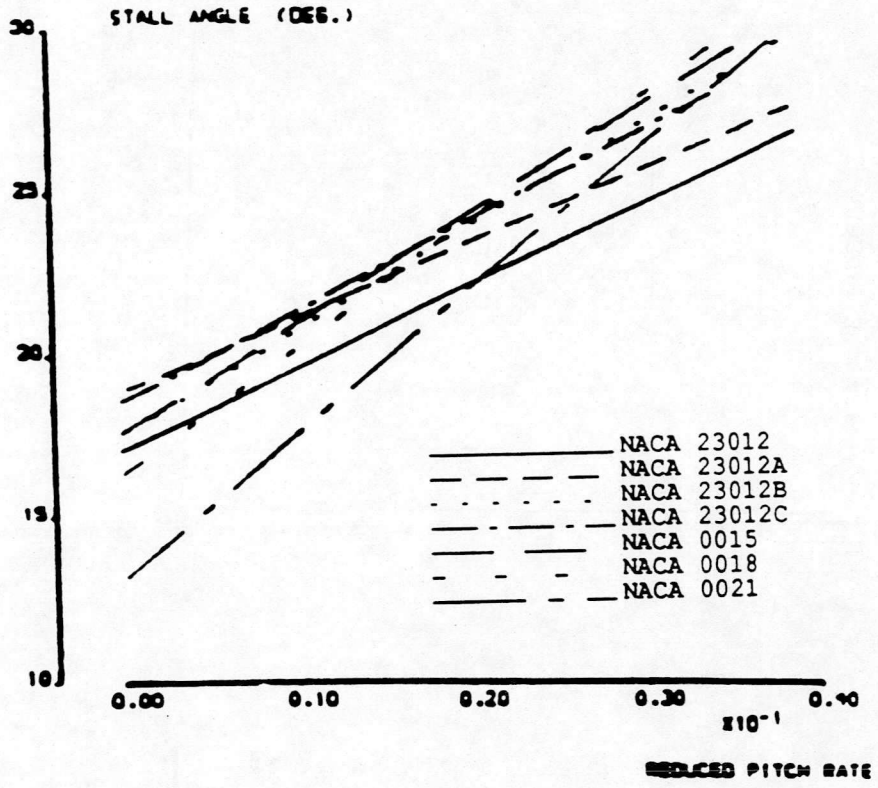

Figure 17 : Variation of C_p deviation incidence with reduced pitch-rate for seven aerofoils at a Reynolds number of approximately 1.5×10^6.

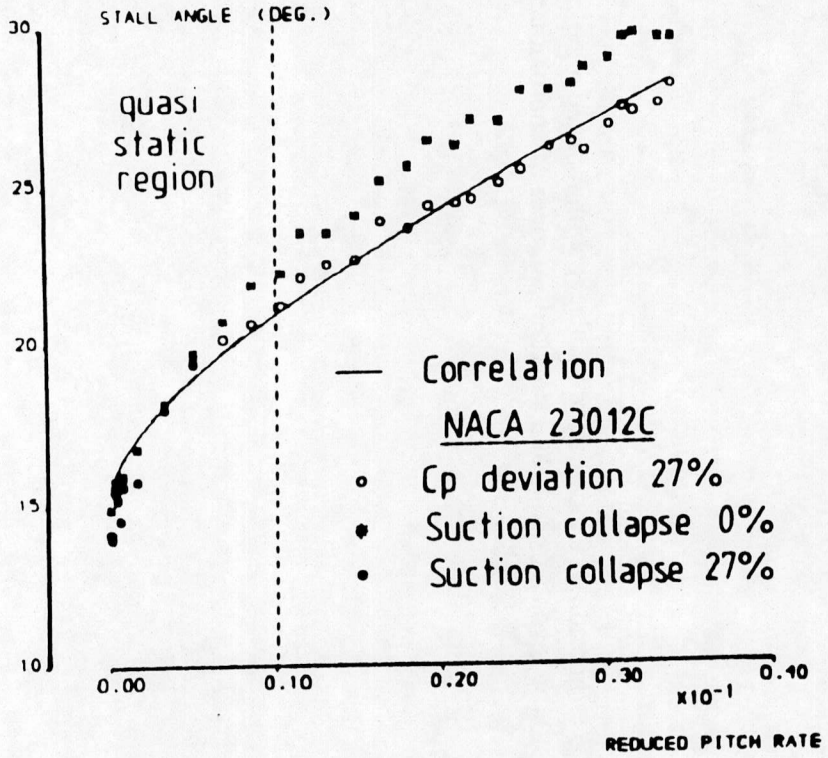

Figure 18 : Comparison between dynamic stall correlation and various chordwise pressure events.

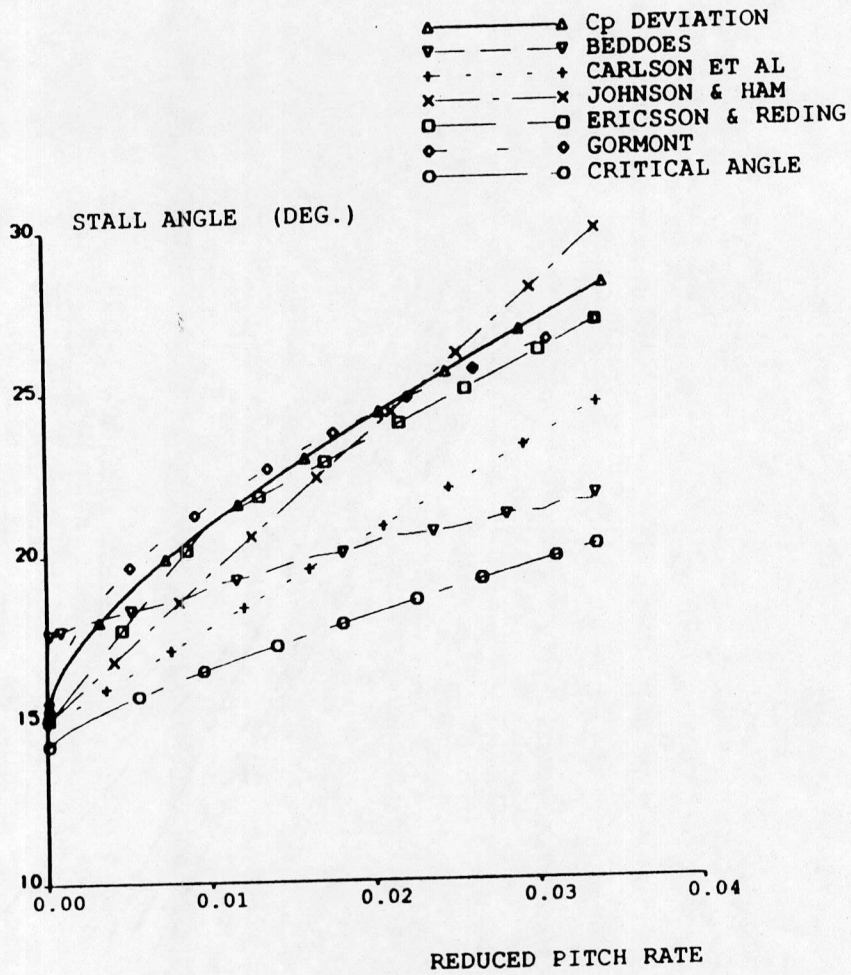

Figure 19 : Comparison between dynamic stall correlation and various established stall criteria.

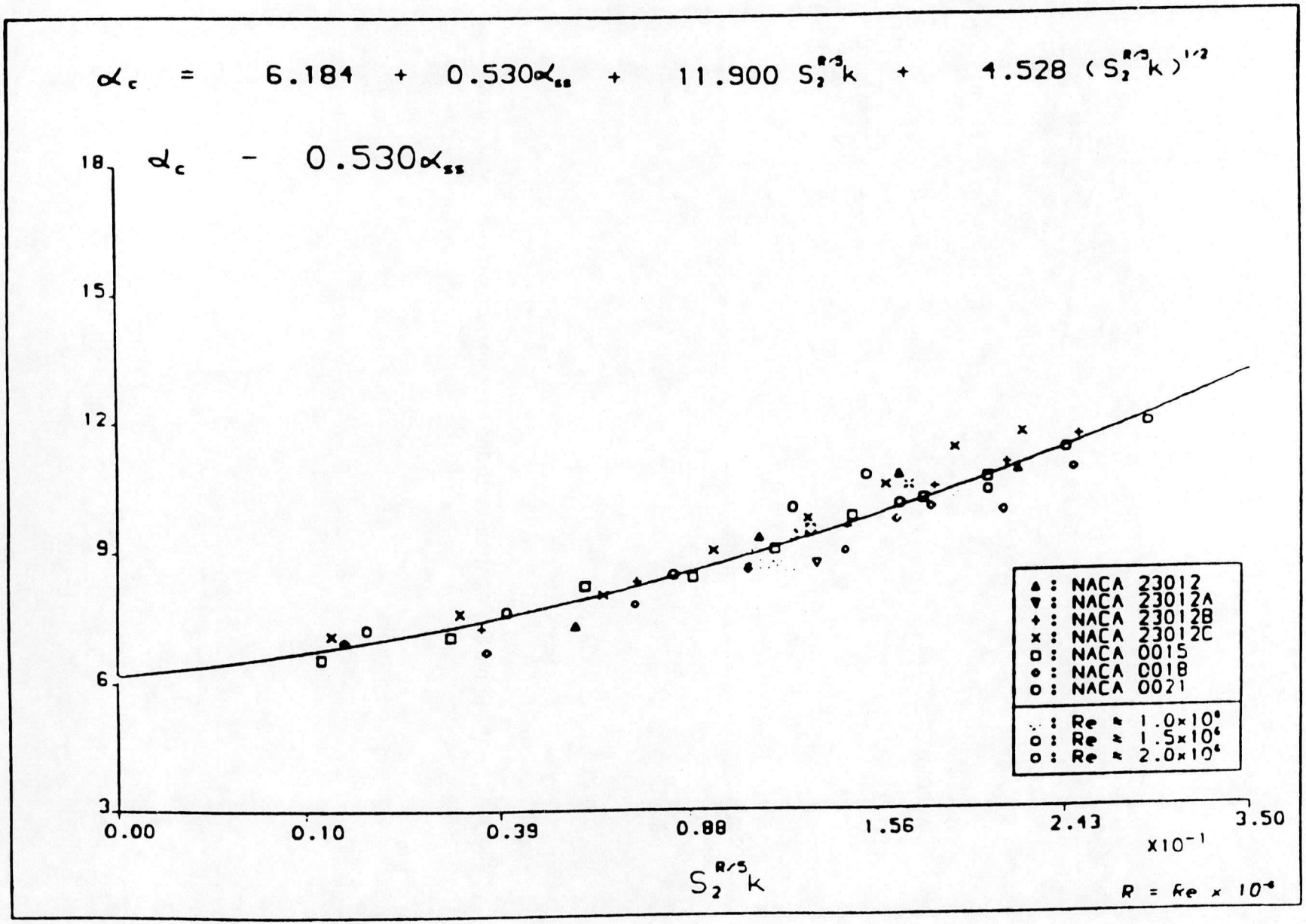

Figure 20 : Correlation of critical angles of attack.

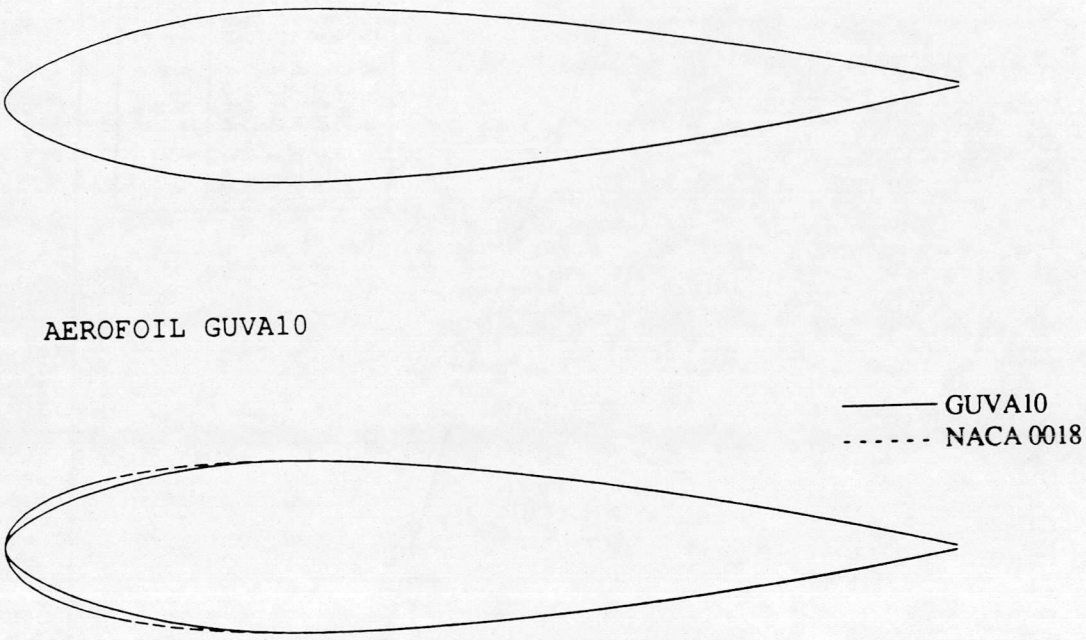

Figure 21 : Profile of the GUVA10 aerofoil, and a comparison with the NACA 0018.

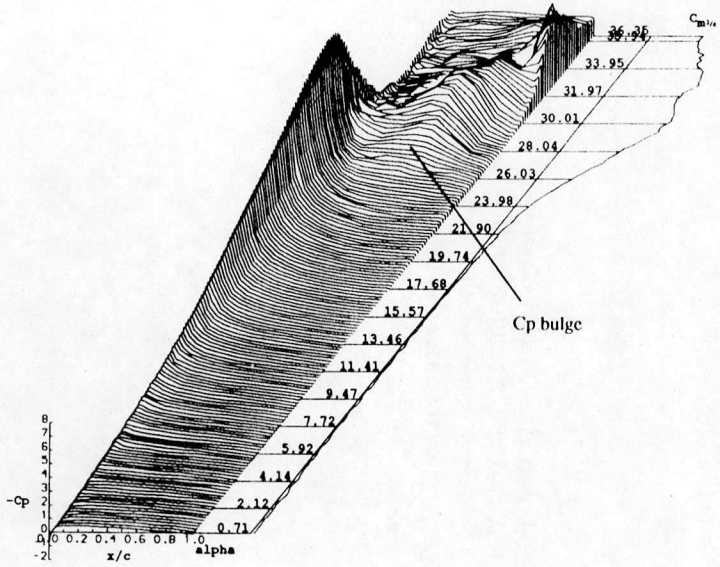

Figure 22a

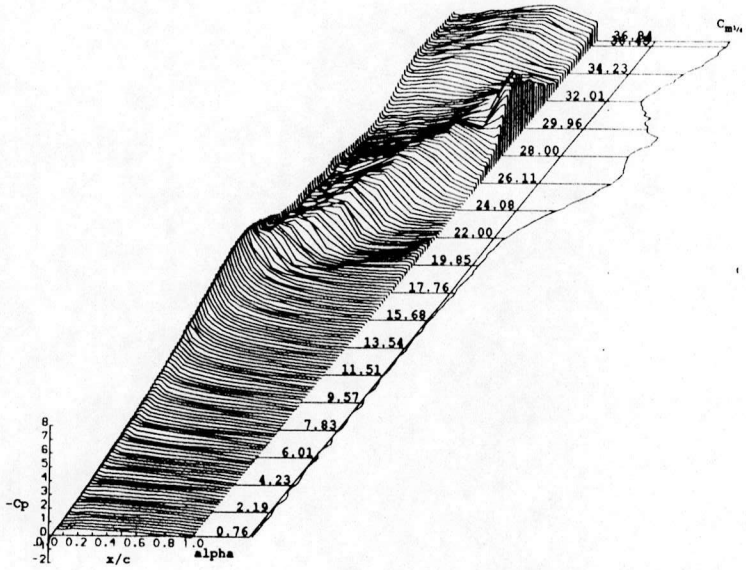

Figure 22b

Figure 22. Development of surface pressures for the high AR NACA 0015 at r=0.0215 and R=1. The clean leading edge case, figure 22a, shows the stall vortex developing around the mid-chord, as indicated, and vortex convection appears as the ridge line. Figure 22b shows pressure data for a test with a roughness strip at the leading edge. The stall vortex develops much closer to the leading edge than for the clean case.

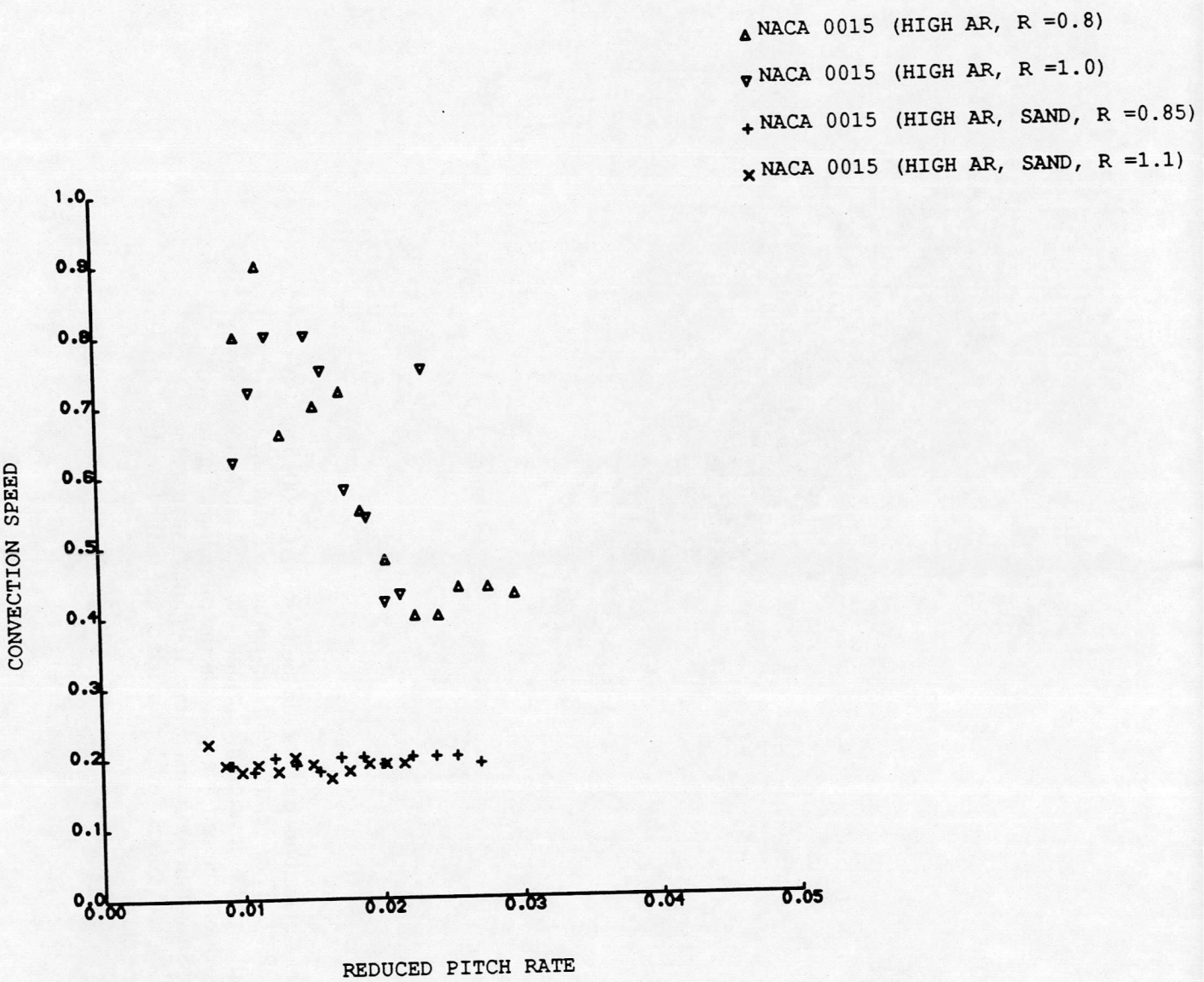

Figure 23. Stall vortex convection speed plotted as a function of reduced pitch rate for the high AR NACA 0015. The clean leading edge data show the speed falling to a constant value, while the data for tests with the leading edge roughness strip show the convection speed to be virtually constant at a value of 19% of the free stream speed.

ENCLOSURES

Angell, R.K., Musgrove, P.J., Galbraith, R.A.McD. and Green, R.B. Summary of the colected data for tests on the NACA 0015, NACA 0018, NACA 0021, NACA 0025 and NACA 0030 aerofoils. Glasgow University Aero Report 9005, February 1990.

Galbraith, R.A.McD. and Coton, F.N. On the passive stall regulation of VAWTs. B.W.E.A. Conference, Norwich, 1990.

Gracey, M.W. The design and low Mach number wind-tunnel performance of a modified NACA 23012 aerofoil, with an investigation of dynamic stall onset. Glasgow University Aero Report 9108, June 1981.

Gracey, M.W. and Galbraith, R.A.McD. An account of the design procedure of aerofoil section GU23012 - MOD B. Glasgow University Aero Report 8608, January 1987.

Gracey, M.W. and Galbraith, R.A.McD. Data for a NACA 23012C aerofoil pitched about its quarter chord axis. Volume I : Pressure data from static and ramp function tests, with photographs of oil-flow visualisation tests. Glasgow University Aero Report 8901, January 1989.

Gracey, M.W. and Galbraith, R.A.McD. Data for a NACA 23012C aerofoil pitched about its quarter chord axis. Volume II : Pressure data from oscillatory tests. Glasgow University Aero Report 8902, January 1989.

Gracey, M.W., Niven, A.J. and Galbraith, R.A.McD. A consideration of low speed dynamic stall onset. 15th European Rotorcraft Forum, Paper Number 11, Amsterdam, September 1989.

Green, R.B., Galbraith, R.A.McD. and Niven, A.J. Measurements of the dynamic stall vortex convection speed. Glasgow University Aero Report 9014, August 1990.

Green, R.B., Galbraith, R.A.McD. and Niven, A.J. The dynamic stall vortex convection speed anomaly : analysis of Lorber and Carta's pressure data. Glasgow University Aero Report 9101, April 1991.

Green, R.B., Galbraith, R.A.McD. and Niven, A.J. Measurements of the dynamic stall vortex convection speed. 17th European Rotorcraft Forum, Paper Number 91-68, Berlin, September 1991.

Horner, M.B., Saliveros, E., Kokkalis, A. and Galbraith, R.A.McD. Results from a set of low speed blade-vortex interaction experiments. Submitted to Journal of Experiments in Fluids, September 1991.

Jiang Dachun and Galbraith, R.A.McD. A new test aerofoil section for vertical axis wind turbines. Glasgow University Aero Report 9012, March 1990.

Niven, A.J. and Galbraith, R.A.McD. Experiments on the establishment of fully attached aerofoil flow from the fully stalled condition during ramp-down motions. 17th ICAS Conference, Stockholm, Sweden, 1990.

PAPERS AND REPORTS IN PREPARATION (abstracts enclosed)

Gracey, M.W., Coton, F.N. and Galbraith, R.A.McD. Design and aerodynamic characteristics of a modified NACA 23012 aerofoil. Part One : Design and characteristics in steady conditions. To be submitted to "Experiments in Fluids".

Gracey, M.W., Coton, F.N. and Galbraith, R.A.McD. Design and aerodynamic characteristics of a modified NACA 23012 aerofoil during contant pitch-rate ramp experiments. To be submitted to "Experiments in Fluids".

Gracey, M.W., Coton, F.N. and Galbraith, R.A.McD. Aerodynamic characteristics of a modified NACA 23012 aerofoil. Part One : Design and characteristics in steady conditions. To be submitted to the "Aeronautical Journal".

Gracey, M.W., Niven, A.J., Coton, F.N. and Galbraith, R.A.McD. A correlation indicating incipient dynamic stall. To be submitted to the "AIAA Journal".